Hourly Wind and Solar Generation Profiles (1980-2019)

PREPARED FOR:
ELECTRIC RELIABILITY COUNCIL OF TEXAS (ERCOT)

Ref. No.: 19-08-027944

ERCOT Region

09 July 2020

CLASSIFICATION
FOR PUBLIC RELEASE

ISSUE
B

AWS Truepower, LLC
463 New Karner Road | Albany, NY 12205 | United States
www.ul.com/renewables

KEY TO DOCUMENT CLASSIFICATION

STRICTLY CONFIDENTIAL	For recipients only
CONFIDENTIAL	May be shared within client's organization
UL INTERNAL ONLY	Not to be distributed outside UL
CLIENT'S DISCRETION	Distribution at the client's discretion
FOR PUBLIC RELEASE	No restriction

DOCUMENT CONTRIBUTORS

AUTHOR(S)	REVIEWER(S)	APPROVED BY
Rojowsky, K. Gothandaraman, A. Beaucage, P.	Rojowsky, K.	Shakarjian, M.

DOCUMENT HISTORY

ISSUE	DATE	SUMMARY
B	07/09/2020	Final Report

TABLE OF CONTENTS

1. Executive Summary 1

2. Introduction and Background 3

3. Atmospheric Modeling, Validation, and Adjustment 5
3.1 Mesoscale Modeling 5
3.2 Resource Adjustment and Validation 6
3.2.1 Wind 6
3.2.2 Solar 7
3.3 Mesoscale-Microscale Modeling 7

4. Wind Generation Profiles 8
4.1 Operational Wind Plants 8
4.1.1 Operational Data Review 9
4.2 Hypothetical Wind Plants 9
4.3 Wind Power Generation 10
4.3.1 Openwind Configuration 11
4.3.2 Openwind Plant Losses 11
4.4 Adjustment and Validation 13
4.5 Wind Power Generation Results 15

5. Utility-Scale Solar Plants 18
5.1 Operational and Planned Solar PV Plants 18
5.1.1 Plant Characteristics 18
5.1.2 Operational Plant Data 19
5.2 Hypothetical Solar PV Plants 19
5.2.1 Near-Current Composite Technology 20

6. Distributed Solar Generation Sites 21
6.1 Simulated Rooftop Generation for Greater Metro Areas 21
6.2 Simulated Rooftop Generation for Rural Regions 22

7. Solar Generation Profiles 23
7.1 Solar Power Generation 23
7.2 Adjustment and Validation 24
7.2.1 Utility-Scale Solar PV 24
7.2.2 Distributed Rooftop Sites 25
7.3 Solar Power Generation Results 26

8. Dataset Usage 30

Appendix A – Operational Wind Plants 33

Appendix B – Hypothetical Wind Plants by County 37

Appendix C – Operational and Planned Utility-Scale PV Plants 1

Appendix D - Hypothetical PV Plants by County 1

Appendix E - Counties in ERCOT CDR Zones 1

LIST OF FIGURES

Figure 3.1: WRF Nested Grids for the Study Domain 6
Figure 4.1: Counties with Operational Wind Plants Modeled 8
Figure 4.2: Counties with Hypothetical Wind Plants Modeled 10
Figure 4.3: Monthly, Hourly and 1-Hour Ramp Distribution of Aggregated Operational Wind Plant Time Series for Concurrent Observed (black) and Modeled (red) Net Power with Correlation Plot (local standard time). 14
Figure 4.4: Probability Distribution Function and Duration Curve of Aggregate Operational Wind Plant Time Series for Concurrent Observed (black) and Modeled (red) Net Power 15
Figure 4.5: Counties Intersecting Hypothetical (blue) or Operational (red) Wind Plants with CDR Zones Outlined 16
Figure 4.6: Aggregated Monthly, Diurnal, and Annual Net Power, 1-Hour Ramp Distribution, and Duration of Net Power Generation for Modeled Wind Plants (local standard time) 17
Figure 4.7: Monthly and Diurnal Modeled Net Power for Operational Wind Plants by CDR Zone (local standard time) 18
Figure 4.8: Monthly and Diurnal Modeled Net Power for Hypothetical Wind Plants by CDR Zone (local standard time) 18
Figure 4.9: Duration of Modeled Net Power Generation for Operational Wind Plants by CDR Zone 18
Figure 4.10: Duration of Modeled Net Power Generation for Hypothetical Wind Plants by CDR Zone 18
Figure 5.1: Counties with Hypothetical PV Plants (shaded) and Operational or Planned PV Plants (triangles), with GHI Resource as Background 20
Figure 6.1: Counties Represented by Rural Profiles 22
Figure 7.1: Hourly Mean Monthly (top left), Diurnal (top right) and Ramp Frequency Distribution (bottom) NCF for an Aggregate of Operational Solar Plants (local standard time) 25
Figure 7.2: Frequency Duration Curve for Operational Solar Plants 25
Figure 7.3: Hourly Mean Monthly (top left), Diurnal (top right) and Ramp Frequency for Aggregated Rooftop Data (local standard time) 26
Figure 7.4: Frequency Duration Curve for Aggregated Rooftop Data 26
Figure 7.5: Areas Represented by Modeled PV Profiles 27
Figure 7.6: Monthly and Diurnal Mean Net Power at a Sample Hypothetical Site modeled as Single-axis (black) and Dual-axis (red) Tracking (local standard time) 28
Figure 7.7: Diurnal Net Capacity Factor for DGPV metro areas 29
Figure 7.8: Comparison of NCF for Aggregated DGPV Austin Metro Area and an Intersecting Hypothetical Site (local standard time) 29
Figure 7.9: Diurnal Net Capacity Factor for DGPV Rural Zones (local standard time) 30
Figure 7.10: Monthly Net Capacity Factor for DGPV Rural Zones (local standard time) 30

LIST OF TABLES

Table 3.1: Model Configuration for WRF runs 6
Table 4.1: Generation Summary by CDR Zone for Operational and Hypothetical Wind Plants 16
Table 5.1: Module Specifications for Near-Current Technology 21
Table 6.1: Distributed PV Assumptions by Intensity of Development 21
Table 6.2: Capacity (MW_{AC}) by Metro Area and Intensity of Development 22
Table 6.3: Rural Distributed PV Capacity by CDR Zone 23
Table 7.1: Static Plant Details for Hypothetical and Distributed PV Sites 23
Table 7.2: Static PV Loss Assumptions 24
Table 7.3: Range of Net Capacity Factors (NCFs) for Modeled Solar PV Time Series 28
Table A.1: Operational Wind Plants in Counties A - Fl 33
Table A.2: Operational Wind Plants in Counties Fl - No 34
Table A.3: Oprational Wind Plants in Counties No - St 35
Table A.4: Operational Wind Plants in Counties St - Wi 36
Table B.1: Count of Sites and Total Capacity by County 37
Table C.1: Operational and Planned Utility-Scale PV Plants in Counties A - Pe 1
Table C.2: Operational and Planned Utility-Scale PV Plants in Counties Pe - W 2
Table D.1: Net Capacity Factor for Hypothetical & Queued Sites in Counties A - La 1
Table D.2: Net Capacity Factor for Hypothetical & Queued Sites in Counties Lo - Z 2
Table E.1: Counties by CDR Zone (Coastal, Houston, North, and Panhandle) 1
Table E.2: Counties by CDR Zone (South and West) 2

1. EXECUTIVE SUMMARY

UL, formerly AWS Truepower (AWST), was retained by the Electric Reliability Council of Texas ("ERCOT" or the "Client") to generate hourly power profiles for 24.0 gigawatts (GW) of operational wind, 30.9 GW of hypothetical wind, 3.4 GW of operational and planned utility-scale solar, 7.0 GW of hypothetical utility-scale solar, and 30.1 GW of distributed PV generation (rural and urban) for the period of January 1, 1980, through December 31, 2019. The purpose of this work is to support ERCOT's various modeling and analysis efforts, and for public dissemination to stakeholders.

Historical meteorological conditions were simulated on a 9-kilometer grid over the state of Texas using the Weather Research and Forecasting (WRF) model to obtain the necessary variables used for power conversion. Model data were adjusted with surface measurements to ensure annual, seasonal, and diurnal mean wind speed and irradiance patterns, including ramping characteristics, are accurately represented. Results show that the adjusted model time series capture the dynamic behavior of annual, monthly, and diurnal wind speeds and solar irradiance. The average wind speed bias is -0.6%. Solar irradiance exhibits an average bias of 2.1%, -7.7%, and 0.3% for GHI, DHI, and DNI respectively.[1.1] Other meteorological variables such as temperature, air density, relative humidity, precipitation, and turbulence intensity were also used to create the power profiles.

Wind and solar plant specifications were compiled from data provided by ERCOT, along with numerous other sources. The plant layouts and other static details of operational plants were used to model each plant as close to reality as possible. Measured generation data was supplied for both wind and solar plants, as well as the plant's estimate of potential generation (without curtailment). The data was filtered and periods of high-quality, uncurtailed generation data were used to validate and adjust the modeled time series at operational wind and solar plants.

Hypothetical wind plants were modeled using the same technology as previously modeled in 2019: 90-meter hub height and wind turbine characteristics anticipated in the 6 to 10-year time horizon. Hypothetical, utility-scale solar PV (single and dual-axis plants), as well as distributed PV, were modeled using an updated PV composite technology representing near-current potential PV generation (i.e., for projects built in the years 2020 – 2025). In general, the trend is for higher wattage and more efficient PV panels; this increase in module rated capacity and subsequent energy density (W/m2) directly increase the PV capacity estimate for distributed generation. The land use and land class data were updated within the four greater metro areas (Austin, Dallas, Houston, and San Antonio). When combined with the increase in energy density, the total metro area rooftop capacity used for modeling increased from 18.4 GW in 2019, to 24.1 GW in the present study. UL also developed a new method to estimate rural distributed rooftop capacity and simulate its hourly generation for each of ERCOT's six Capacity, Demand, and Reserves (CDR) zones.

Hourly wind power profiles were generated at 150 operational and 148 hypothetical sites with Openwind, UL's plant design and optimization software used for high fidelity energy production estimates. The adjusted WRF time series, operational plant characteristics, and next-generation wind technology at hypothetical plants were used to simulate hourly, net wind power generation for two scenarios. The first scenario includes only operational plants. The second scenario includes both operational and hypothetical wind farms, so that hypothetical profiles include the effect of additional wake losses from nearby operational wind plants.

[1.1] GHI is defined as the total solar radiation received on a surface horizontal to the ground. GHI is the sum of direct normal irradiance (DNI) and diffuse horizontal irradiance (DHI). The DNI component is the radiation received perpendicular to the sun's rays. The DHI component is radiation that is received indirectly from the sun via scattering by the atmosphere.

The modeled wind generation at operational plants was adjusted to account for non-standard and site-specific plant losses, such as turbine availability or power curve derating behavior that were not explicitly modeled in Openwind. At each plant, an adjustment was developed using concurrent observed and modeled generation data. For operational plants with an insufficient data record, a composite adjustment was developed and applied. No adjustment was made to the hypothetical profiles.

The final power generation results were evaluated for reasonableness and compared to historical wind generation. The net capacity factor (NCF) of the modeled generation time series range from 21.1% to 52.1% for the operational plants, and 31.3% to 53.4% for hypothetical plants. The final dataset has a bias of less than 1.0% and an hourly coefficient of determination (R^2) of 0.89 for the aggregate generation. The modeled wind generation time series are shown to well capture the seasonal and diurnal cycle of observed generation, as well as the ramping behavior.

Hourly solar generation was simulated using the adjusted WRF modeled time series and UL's power conversion software at 35 utility-scale operational, 139 hypothetical plants (single and dual), and aggregate sites of distributed rooftop generation (representing the four greater metro areas and six rural aggregates by CDR zone). The profiles of hypothetical, operational, or planned utility-scale solar plants that did not have sufficient generation data for custom adjustment were adjusted using a composite adjustment developed from all operational solar plants. For the distributed rooftop generation profiles, a composite matrix was developed using recent historical rooftop generation data from zip codes in each of the metro areas.

Results show that the overall PV generation values align well with expectations on a monthly, diurnal, and overall annual basis, and ramping statistics appear to reasonably depict fluctuations in power generation. The operational plants have mean NCFs ranging from 18.7% to 31.0%, with an aggregate bias of 0.0% on generation and an hourly coefficient of determination (R^2) of 0.92. Generally, the distributed PV profiles exhibit lower NCFs than the utility-scale PV plants. Even when accounting for local irradiance resource, generation varies between centralized, utility-scale and distributed rooftop generation due to plant characteristics. The net capacity factor of distributed rooftop generation in the urban areas varies little across the different land use classes (14.9 to 15.4%), while the rural profiles exhibit a wider range of NCFs spanning 14.5 to 20.4%. The effect of longitude can be seen in the mean diurnal NCF for both urban and rural profiles, where sites in the east reach higher generation earlier in the morning, followed by sites further west. The opposite pattern, although less well pronounced, is seen in the afternoon. The distributed generation profiles for the greater urban and rural areas have a bias of -1.1% on generation and an hourly coefficient of determination (R^2) of 0.94.

2. INTRODUCTION AND BACKGROUND

UL has collaborated with the Electric Reliability Council of Texas (ERCOT) since 2012 to simulate hourly generation profiles for both operational and hypothetical wind capacity across its service territory. Modeling wind and solar generation fleets is a challenging task that seeks to balance the required model inputs with an efficient process to reproduce plant behavior that aligns with historic weather patterns. This requires the use of state-of-the-art modeling techniques that are updated continuously as industry knowledge expands and rapidly evolves. Over the past eight years, new methods have been applied in the development of ERCOT's hourly generation profiles including updated or new atmospheric models, initialization data, resource assessment methods, power conversion software tools, and adjustment processes. Understanding the similarities and differences between methods used to create each version of profiles is important to its application, and therefore references to previous work are provided throughout this report.

The first series of wind profiles simulated historical wind power for the period of 1997 – 2012, with annual updates provided through 2016, using consistent power conversion methods and composite power curves. In 2015, UL began using the Weather Research and Forecast Model (WRF) to simulate the hourly atmospheric variables, and previous wind profiles were recreated (1997-2014) using the variables from WRF as input to UL's power conversion method. All other wind resource assessment and power conversion processes and specifications remained static. This dataset was updated annually until 2017 using the same methods and input parameters by appending new model data and converting it to power. In 2018, a set of hourly wind profiles was provided using operational plant specifications, as available, and the then-current (2017) fleet configuration as applied to an extended historical weather record (1980-2017). Operational and hypothetical utility-scale solar PV plants, and distributed generation profiles based on land use classes in four major urban areas (Austin, Dallas, Houston, and San Antonio) were also modeled in 2017.

The 2020 profiles (1980-2019) provide long-term time series of hourly production (without curtailment) at operational wind and solar plants based on current fleet characteristics, as well as generation at hypothetical sites using near-current technology. In addition, distributed generation profiles representative of the potential rooftop generation in the rural areas of ERCOT's six CDR zones were provided.

Current methods were applied to convert the meteorological conditions into hourly power for 24.0 GW of operational wind, 30.9 GW of hypothetical wind, 3.4 GW of operational and planned solar, 7.0 GW of hypothetical utility-scale solar, and 30.1 GW of distributed PV generation for the period of January 1, 1980, through December 31, 2019. This report summarizes the methods and results and is divided into eight main sections:

Section 3 describes the methods used to develop the modeled atmospheric time series using a state-of-the-art Numerical Weather Prediction model for each operational and hypothetical location. Resource validation and adjustment are described, as well as new initialization data and the application of a microscale model for wind.

Section 4 describes the wind power conversion process using Openwind, a state-of-the-art wind resource assessment and optimization software, including the plant specifications used as input for operation and hypothetical plants, operational data available for validation, and the results.

Section 5 describes the specifications used for operational and hypothetical (single and dual-axis tracking) solar PV plants, the composite technology applied, and the operational data available for validation.

Section 6 describes the method used to identify the potential rooftop generation across metro and rural areas.

Section 7 summarizes the validation and results for the operational and hypothetical utility-scale solar PV plants, as well as the distributed PV urban and rural aggregate profiles.

Section 8 provides end-users with a summary of assumptions and potential sources of bias in the hourly profiles to help guide their future use and application.

3. ATMOSPHERIC MODELING, VALIDATION, AND ADJUSTMENT

3.1 Mesoscale Modeling

Historical meteorological conditions were simulated over the state of Texas using the Weather Research and Forecasting (WRF) model,[3.2] a leading open-source numerical weather prediction (NWP) model that simulates the fundamental physics of the atmosphere including radiation, land surface-atmosphere interactions, planetary boundary layer (PBL) turbulence, microphysics, and cloud convection. WRF solves the fully compressible, non-hydrostatic Navier-Stokes equations (i.e., conservation of mass, momentum and energy) and utilizes a complete suite of physics parameterization schemes. WRF contains 11 boundary layer schemes, 18 microphysics schemes, and 10 convective parameterization schemes, as well as a three-dimensional grid to simulate atmospheric processes. The 3D grid can cover a large area, such as a province or state, a country or the globe depending on the grid resolution; a coarser grid can cover a larger area with the same number of grid cells. The vertical levels of NWP models extend far into the stratosphere, typically up to 50 millibar (mb), which is roughly equivalent to 20.5 kilometers (km) in altitude, in order to capture the jet stream. Mesoscale numerical weather prediction models – the same models used for weather forecasting – are the best tools available to simulate evolving atmospheric conditions, especially at the synoptic and meso scales[3.3].

Input into the WRF model includes a variety of online, global geophysical and meteorological databases. ERA5, the fifth-generation reanalysis dataset provided by the European Center for Medium Range Weather Forecasting,[3.4] supplied the model initialization and boundary conditions. These data provide a snapshot of atmospheric conditions around the world at all levels of the atmosphere and were ingested into the WRF model every three hours. High-resolution terrain, soil, and vegetation data were also used as input where available.

WRF simulations were carried out to model the atmospheric circulation for the 1980 to 2019 study period to obtain the variables necessary to estimate wind and solar power production at each site. WRF was set up to run two nested grids simultaneously over the project area with a horizontal grid spacing of 27 and 9 km (Figure 3.1). In essence, different scales of motion are resolved by grids with different resolutions. A ratio of 3 between the parent and child grid resolution (i.e., 27 vs. 9-km) ensures a proper energy cascade from the large scales to the small scales, which is mainly due to the non-linear interactions. The two grids at 27-km (shown in red) and 9-km (shown in green), respectively, resolve successively finer scales across the whole region. The 27-km grid passes the boundary conditions to the innermost 9-km grid, which modifies the atmospheric circulations in response to a consistent set of surface forcings from the terrain elevation, land cover, soil temperature, and moisture, etc. In other words, the data is passed from one grid to the next in a way that allows the model to develop the finest scales in a consistent manner. The final model simulation includes both the ERCOT service area and nearby adjacent land areas to provide a complete dataset for the period of 1 January 1980 to 31 December 2019. Simulated meteorological values required for solar PV and wind power production models were retained on an hourly basis. The model configuration used in this study is summarized in Table 3.1.

[3.2] Skamarock, W. C., Klemp J.B., Dudhia J., Gill D.O., Barker D.M., Duda M.G., Huang X-Y., Wang W. and Powers J.G. A Description of the Advanced Research WRF Version 3. Boulder: NCAR Technical Note NCAR/TN-475+STR, 2008.

[3.3] The synoptic and meso scales of planetary motion corresponding to weather features on the order of several hundreds to several throusands of kilometers (e.g., common high and low pressure systems), or for smaller features ranging from a few kilometers and up to several hundred kilometers (e.g., thunderstorms, or land and sea breezes), respectively.

[3.4] Available at: https://www.ecmwf.int/en/forecasts/datasets/reanalysis-datasets/era5

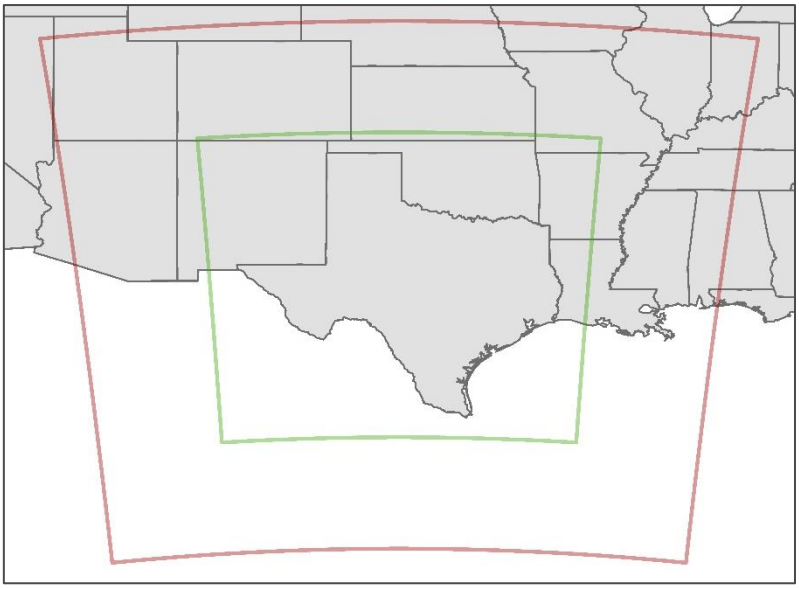

Figure 3.1: WRF Nested Grids for the Study Domain

Table 3.1: Model Configuration for WRF runs

Model	WRFv3.5.1
Initialization Data Source	ERA5
Spatial Resolution (Innermost Grid)	9 km
Frequency of Data Sampling	Hourly
Data Assimilation	Spectral Nudging
Planetary Boundary Layer Scheme	Mellor-Yamada-Janjic Scheme

3.2 Resource Adjustment and Validation

Before converting the modeled meteorological time series to plant production, it is first necessary to correct for biases to ensure that the modeled wind and solar resource used in the conversion to power is accurate. This is done by scaling the WRF meteorological variables to match the expected resource average and resource variability at each site. The adjustment and validation of model data require a sufficiently large sample of observed data to tune the modeled variables to observed values.

3.2.1 Wind

Data from tall towers within the modeling domain were used to adjust the WRF-derived wind speeds. The measured data were quality-controlled, including, but not limited to ensuring data were not suspiciously below or above the expected wind speed thresholds, comparing measurements at redundant sensors, and performing analyses to examine suspect trends. Datasets were discarded if they did not pass the quality-control tests, have a sufficient period of record (at least one year), or provide meaningful values for validation and adjustment. Some datasets were truncated to a period that was considered valid. These data were then used to validate and adjust the final atmospheric dataset used in the power production models.

The final observed dataset used in the adjustment process consisted of 10-minute data from 40 towers, for a total of over 200 years of data which increases confidence in the accuracy of resource characterization at the sites being modeled. UL compared the hourly WRF meteorological time series against the observed measurements for the concurrent period examining the annual, monthly, and

diurnal pattern. The simulated WRF time series correlated well with the observations, which were primarily used to adjust diurnal wind speeds in the modeled time series. Most towers (36 of 40) are located in Texas. Four towers from neighboring areas of New Mexico and Oklahoma were also included. These tall tower data were used to adjust diurnal mean patterns in the modeled hub-height wind speed time series. Results show that the adjusted model time series capture the dynamic behavior of annual, monthly, and diurnal wind speeds, with an average bias of -0.6%. The adjusted WRF wind speed and other meteorological variables such as temperature, air density, relative humidity, precipitation, and turbulence intensity served as inputs to the Openwind software used to create the power profiles.

3.2.2 Solar

High-quality surface stations with solar irradiance measurements (both GHI and components, when available) were used to validate and adjust the modeled irradiance time series. The measured data were quality-controlled, which included but was not limited to: correcting for negative nighttime irradiance values, ensuring data were not suspiciously below or above the expected clear sky irradiance values, comparing measurements at redundant sensors or nearby stations, and performing analyses to examine suspect trends. Datasets were discarded if they did not pass the quality-control tests, have a sufficient period of record, or provide meaningful values for validation and adjustment. Some datasets were truncated to a period that was considered valid.

Data from 16 reference stations were compiled and used to adjust the modeled irradiance resource (totaling over 155 years of valid hourly observations). The frequency distribution of the modeled irradiance time series was adjusted to better reflect the distribution of observed values. This process adjusts both the means and the extremes of modeled irradiance data and results in a more accurate representation of clear, partly cloudy, and cloudy days. The adjustment reduced the annual irradiance bias at all sixteen validation stations to well within reasonable limits (and measurement uncertainty), resulting in an average bias of 2.1%, -7.7%, and 0.3% for GHI, DHI, and DNI respectively. The root-mean-squared error (RMSE) after adjustment is 3.6%,10.9%, 4.7% for GHI, DHI, and DNI.

3.3 Mesoscale-Microscale Modeling

The accurate prediction of a wind plant's energy production is dependent upon a detailed understanding of the spatial distribution of the wind resource across the project area. UL independently pioneered a method to couple a mesoscale model and a microscale model to characterize the wind resource at spatial resolutions on the order of 10 to 100 meters.[3.5] UL's modeling system, known as SiteWind, relies on a mesoscale model to properly simulate the atmospheric flow up to the meso-gamma scales (~1 km) then the mean wind flow modeled by the mesoscale model is downscaled to a 200-m grid spacing using a diagnostic mass-conserving model called WindMap. The WindMap model is a mass conserving model that ingests mesoscale NWP model outputs and computes the three-dimensional wind field. WindMap attempts to retain as much information as possible from the mesoscale NWP model while accounting for the high-resolution terrain elevation and land cover data. The WindMap model outputs are stored in binary wind resource grid (WRB) files, which are later used by the Openwind software to extrapolate the adjusted WRF meteorological time series to the turbine sites and estimate wind power generation.

[3.5] Brower, M.C. (1999). Validation of the WindMap Program and Development of MesoMap. Proceedings from AWEA's WindPower conference. Washington, DC, USA.

4. WIND GENERATION PROFILES

4.1 Operational Wind Plants

Wind plant details were compiled in order to ensure completeness and accuracy of the ERCOT wind fleet to be modeled. ERCOT provided wind resource registration[4.6] data for individual wind unit codes, their installed capacity, wind turbine specifications, and centroids of the units. This information was reviewed for consistency and compared to information derived from outside sources. A total of 150 plants were modeled, representing all RARF unit codes provided. Of the 150 plants, 10 had not been previously modeled by UL. These plants achieved commercial operation between late 2018 and the end of 2019. A summary of all operational plants modeled can be found in Appendix A, and the counties represented by the 150 operational units are highlighted in Figure 4.1 (the nine counties which contain the 10 new plants are shaded dark red). For each wind plant, the layouts were verified based on static plant details and aerial imagery, when possible. Historical generation data was used to verify plant capacity assumptions of operational plants.

Each plant's turbine model and the manufacturer's power curve was used to simulate the operational unit at the installed hub heights.[4.7] Plant-specific power curves were not available. For some units, the RARF turbine megawatt (MW) ratings were slightly higher than the manufacturer's standard power curve ratings (representing a particular power mode variant). For these unit codes, custom power curves were developed to best approximate the expected behavior of the particular power curves needed. No information was available about the use of turbine power curve de-rating strategy at wind sites with extreme high temperature or elevation.[4.8] The modeled plant profiles were validated and adjusted using the highest granularity of historical generation possible, which varied amongst operational plants based on the amount of measured data available.

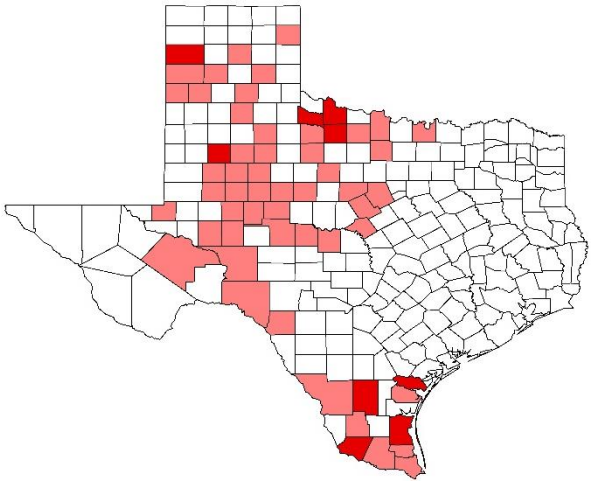

Figure 4.1: Counties with Operational Wind Plants Modeled

[4.6] Data was provided from the RARF (Resource Asset Registration Form) database, which contains static details for power plants as provided to ERCOT from the developer, plant owner, or operator. The wind plant RARF data received were dated 01/29/2020. ERCOT provided RARF data to UL pursuant to Nodal Protocol section 1.3.6(1)(h), Protected Information disclosure to vendors.

[4.7] Previously, wind profiles were provided at the turbine hub heights rounded to the nearest 5 meters (a total of 10 unique hub heights). For this study, operational plants were modeled at the hub heights specified in the RARF data (16 unique hub heights).

[4.8] This can result in artificially high power generation, particularly during the hot summer months.

4.1.1 Operational Data Review

Operational wind plant data was reviewed to determine the valid data outside of the "break-in" period of each individual plant, which was subsequently used for modeled time series adjustment. UL assumes a typical break-in period of four months (minimum) before turbines are running at peak efficiency. Of the 150 operational plants, 142 wind plants were considered by UL as being past their break-in period.[4.9] Only those with at least one year of operational data past the break-in period were adjusted and validated using their plant-specific generation data (a total of 142 plants). Eight plants were not mature enough to provide meaningful actual power generation for the modeling process. The eight operational wind farms within their break-in period were: Sites 3000 to 3006, and 3009.

Historical, hourly generation data from operational plants were used to adjust the modeled plant profiles to account for turbine and plant underperformance, plant availability, power curve variants, generator heating or cooling packages, and other plant-specific losses that cannot be explicitly modeled. The historical generation data includes the actual, measured power generation (including plant losses and curtailment), and the high sustainable limit (HSL) for each hourly record. [4.10] The HSL refers to the limit established by the plant owner/operator (qualified scheduling entities) that describes the maximum sustained energy production capability of the plant at that time. In essence, the HSL reflects the expected, uncurtailed power generation at actual plant availability. UL used the greater of the observed power and the HSL as the valid "historical" data to be used in validation and model adjustment.

The HSL data was screened and filtered before being used in the modeling process. The break-in period was filtered out of the historical generation data, and the remaining time series at each plant was quality controlled as follows. Historical power generation in excess of the plant capacity range was discarded. Data records were discarded if the generation read a constant value, including 0 MW, for 24 consecutive hours or more (a likely indication of data transmission issues). Although most periods of no generation for a full 24-hour cycle (i.e., 0 MW for the whole plant) was observed during the "break-in" period, an automated QC procedure may have misrepresented the net capacity factor at some plants by discarding valid plant outage data.

Lastly, the potential for upstream wake effects from neighboring farms was considered when finalizing the HSL dataset used in the modeling process. Since the wind power conversion process assumes all operational plants are installed throughout the modeling period (1980 – 2019), and because the historical generation data are used to adjust modeled output at these wind farms to account for plant-specific losses, it is important to only consider the period of data after which all upstream wind farms were built (the "fully waked period"). The date of the most recently installed upstream wind farm was used as the start of the fully-waked period for plants that were identified as "waked".

4.2 Hypothetical Wind Plants

UL used a Geographical Information System (GIS)-based approach to identify development constraints and build out potential sites for utility-scale wind generation across the ERCOT region. UL leveraged the previous site screening results and worked with ERCOT to identify additional areas of favorable wind power development to be represented by modeled generation profiles.[4.11] In total, 30.9 GW of utility-scale hypothetical wind sites were selected for modeling based on their gross wind generation

[4.9] A visual inspection of the generation data was carried out for each plant to determine the break-in period. At some plants, up to six months of initial generation data were discarded because of data discontinuity with the remainder of the record; e.g., no data, low data recovery, or unusual fluctuations in power generation.

[4.10] New measured data was incorporated for plants which had < 1 year of data in the previous 2018 analysis.

[4.11] Rojowsky, K, Johanson, C., Filippelli, M., Gothandaraman, A., Frank, J., Beaucage. 2019. Site Screening and Hourly Profiles. Prepared for the Electric Reliability Council of Texas. Technical Report prepared for ERCOT by UL. Reference number 18-01532

potential, geographic distribution, and other factors; this consisted of 148 plants at 100-400 MW each (Appendix B).

The hypothetical sites in this study include those previously modeled in 2019, and 20 more sites (with an additional 4.5 GW of capacity). Of these 20 new sites, 13 neighbor operational wind plants at a distance likely subjecting them to upstream wakes from the operational plants.[4.12] The counties which encompass the 148 hypothetical plants are highlighted in Figure 4.2 (the 15 counties which contain the twenty new sites are shaded darker blue).

UL reviewed the turbine technology assumptions made for 2019 hypothetical plants and found no appreciable difference in wind turbine technology for the 6 to 10-year time horizon. As a result, the hub height modeled for hypothetical wind plants remained at 90-meters. For the previous study, UL had developed two composite power curves with which to model hypothetical sites: a primary power curve (applicable for a broad range of sites) and a secondary power curve with more robust design limits (used to model wind power generation at more energetic sites).[4.13] For the present study, all hypothetical plants were modeled with one power curve based on the plant-array average, free stream wind speed (i.e., most wind speed sites with the primary power curve and high wind speed sites with the secondary power curve).

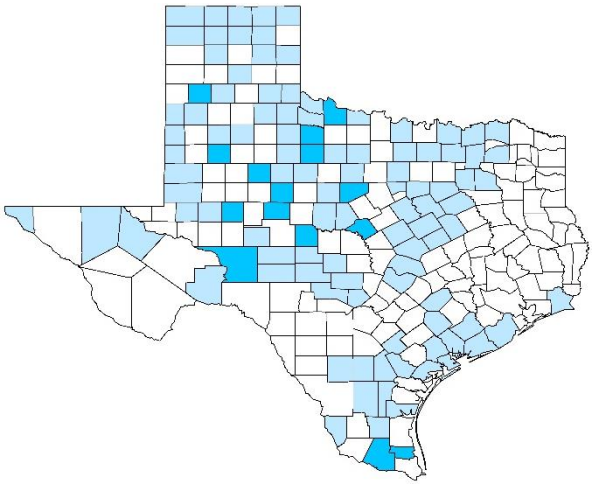

Figure 4.2: Counties with Hypothetical Wind Plants Modeled

4.3 Wind Power Generation

Hourly wind power profiles were generated at 150 operational and 148 hypothetical sites. The adjusted WRF time series (Section 3.2) served as input to Openwind, UL's plant design and optimization software used for high fidelity energy production estimates. Operational plant characteristics (Section 4.1) and next-generation wind technology at hypothetical plants (Section 4.2) were used to simulate hourly wind power generation across all sites. The following section describes the Openwind setup and configuration used to simulate gross and net energy production, as well as plant losses.

[4.12] The use of Openwind, UL's plant design and optimization software allows plant-on-plant wakes from upstream operational plants to be directly modeled at the hypothetical sites.

[4.13] In 2019, sites with average winds speeds of > 8.5 m/s were modeled with two power curves, primary and secondary.

4.3.1 Openwind Configuration

Openwind requires the following data and information to calculate the wind power generation across turbines in the model domain: data files describing the spatial and temporal distribution of the wind resource, information about the local terrain, and a set of parameters describing wind turbine characteristics at each site. Spatial and temporal distributions of the wind resource were ingested in the form of binary wind resource grids (WRBs) and hourly WRF meteorological time series. The WRBs generated by UL's coupled mesoscale-microscale modeling system (Section 3.3) defines the wind resource at multiple heights above ground level across all the project locations. The terrain elevation and surface roughness maps are those used in the microscale WindMap simulations. Turbine characteristic files were created for each of the operational and next-generation turbines; these files include parameters for the hub height and rotor diameter, power and thrust curves, cut-in, cut-out, and cut-back-in wind speeds, and extreme temperature shutdown.[4.14]

After running the wind resource model, the WRB is imported into Openwind to define the wind resource for the project area. An adjusted WRF meteorological time series (Section 3.2) from each wind plant was imported into Openwind as a "virtual meteorological mast" to adjust the resource grid. The Weibull distribution parameters in the WRB are converted into directional speed-up ratios relating the wind speed at each grid point to the virtual met masts. Openwind adjusts the wind speed and direction distribution in WRBs to match those at the virtual met mast locations and applies a temperature adjustment based on terrain elevation. That way, time series of wind resource and ancillary variables are extrapolated to each turbine location. This allows for the time series of weather conditions to vary between turbines, while the wind field in the resource grid is preserved at each time step. For example, turbines at higher elevations typically experience lower temperatures, lower air density, and corresponding environmental losses (Section 4.3.2).

The Openwind time series energy capture module runs the meteorological time series through the respective power curve at each turbine to estimate gross wind power generation, adjusting for the effects of turbulence intensity and air density on the power curve. Data from adjacent heights are used within Openwind for extrapolating to any turbine-specific hub heights that are between these mesoscale model levels. Details of the energy loss calculations to estimate net power are given in the following section.

The time series energy capture module was run for two scenarios. The first scenario included only operational wind farms, so that the operational plant profiles did not include wake effects of hypothetical sites. The second scenario included both operational and hypothetical wind farms; this allowed hypothetical plant profiles to include wake losses from nearby operational plants.

4.3.2 Openwind Plant Losses

The net energy production is derived by subtracting all the wind plant losses from the gross energy by turbine and represents the total power at the electrical connection point of the wind farm to the grid (typically a substation). UL estimated gross and net energy production, including losses for the following categories: wake, availability, environmental, and electrical. Losses not included in this simulation were: blade degradation, curtailment, temperature de-rating, and turbine performance. Blade degradation is marginal and difficult to estimate accurately and therefore omitted. All profiles were modeled with no grid curtailment losses. UL did not have a clear indication of turbine performance issues in the ERCOT territory or turbine de-rating behavior and therefore assumed that the power generation of all turbines followed their advertised power curve. However, the final, adjusted model profiles at operational plants

[4.14] No hot or cold weather packages were assumed.

account for plant-specific turbine performance losses because of their adjustment to historical HSL data (which reflects the theoretical, uncurtailed power generation). No force majeure was considered.

UL uses the Deep Array Wake Model (DAWM) inside Openwind to calculate wake losses.[4.15] The DAWM is comprised of two separate wake models operating independently: (1) the Eddy Viscosity model (based on the Navier-Stokes equations rate of wake dissipation)[4.16] and (2) a model designed to better capture wake losses in deep (multi-row) arrays of wind turbines.[4.17] In combining the two models, the DAWM implicitly defines "shallow" and "deep" zones within a turbine array. In the shallow zone, the direct wake effects of individual turbines dominate, and the unmodified Eddy Viscosity (EV) model is used to calculate wake deficits; in the deep zone, the deep-array effect is more prominent and a surface roughness-based model is employed.

In addition to wake effects from turbines within the same wind farm (i.e. internal wakes), the turbine-induced wakes from neighboring wind farms located upstream can impact the energy production at any particular plant. Openwind is able to capture these plant-on-plant wake losses (i.e. the "wind farm shadowing effect").

Time-varying wind plant availability was modeled in the Openwind software using a Markov chain method.[4.18] The availability model simulates the change in the number of turbines that are available to generate power from one time step to the next. Availability losses occur when some turbines in a project, or the entire project, are unavailable for some reason when they could be generating power. This can occur due to turbine faults or a failure of one or more turbine components. It can also be caused by a failure or shutdown of the power grid or substation. Plant start-up problems, repair delays, fleet-wide turbine retrofits, or systemic operational issues can cause extended periods of downtime that reduce the long-term average availability. An average availability loss of 2-10% is typically encountered in operations[4.19] and can vary widely amongst plants.

The main component of the Markov chain is a transition matrix, which indicates the probability of transitioning from any given current state to any other state in the next time step. In Openwind, for a given availability state, specific turbines are selected at random to be switched off. This allows the effect of availability on wake losses, for example, to be correctly modeled. From one time step to the next, only the minimum number of turbines that need to be switched on or off to arrive at the next availability state is selected in order to model the persistence of turbine downtime patterns. To prevent wind turbines from going on and off constantly in an unrealistic way, once a turbine is shut down due to maintenance or an outage, the model keeps it down until the availability rises enough that it must be turned back on.

Various environmental losses are calculated in Openwind using the WRB-adjusted resource time series at each turbine location. These losses include low and high-temperature shutdowns, and high wind hysteresis. Openwind models the low- and high-temperature shutdown or power curve derating behavior for each turbine type using several wind turbine control set points such as the minimum and maximum threshold, if available and applicable. High wind hysteresis is accounted for using the waked

[4.15] Brower, M. C. and N. M. Robinson, (2012) The Openwind Deep Array Wake Model – Development and Validation, Technical report from AWS Truepower, Albany (NY), USA. 16 pp.

[4.16] "Openwind Theoretical Basis and Validation. Technical report from AWS Truepower, Albany (NY), USA. 26 pp.

[4.17] Loosely based on Frandsen, S.T. (2007). "Turbulence and Turbulence-Generated Structural Loading in Wind Turbine Clusters". Technical report from the DTU Wind Energy (Risø-R-1188), Roskilde, Denmark. 130 pp.

[4.18] Plant availability includes planned and unplanned turbine outages, grid or substation shutdowns, and any repair or restart times.

[4.19] Brower, M.C. et al. (2012). "Wind Resource Assessment: A Practical Guide to Developing a Wind Project". Wiley, 296 pp.

wind speeds and the appropriate cut-in and cut-out speeds, as well as power curve derating, for each turbine type.

Electrical losses are experienced by all electrical components of a wind farm, including those from the padmount and substation transformers, electrical collection system, as well as turbine power consumption, including any hot or cold weather packages. The electrical efficiency of a wind farm is primarily driven by losses associated with the transformers and the collector system. The Openwind software includes an electrical efficiency model derived from operational data that simulates this behavior. Turbine power consumption consists of electricity used to run equipment such as yaw mechanisms, blade-pitch controls, aircraft warning lights, oil heaters, pumps, etc. The sum of these sources of turbine power consumption is typically much less than 1%.[4.20] The Openwind software includes a turbine consumption model derived from operational data to account for these losses.

4.4 Adjustment and Validation

The model generation time series were adjusted using the filtered, historical generation data from operational plants[4.21] to more accurately reflect real power generation patterns. The main purpose of this adjustment is to account for non-standard and site-specific plant losses, such as turbine availability or power curve derating behavior that were not explicitly modeled in Openwind. For the final adjustment process, correction matrices were developed based on historical and modeled power generation at each plant. These matrices are two-dimensional scaling factors by power generation bin and month. The plant-specific matrices were used to adjust the power generation time series at each operational plant with at least one year of observed data. For the eight operational plants with insufficient data record (see Section 4.1.1), a composite adjustment was developed from data at the other 142 plants. No post-processing adjustment was applied to the hypothetical wind plant profiles.

The final generation profiles were examined for reasonableness at the plant level and as an aggregate. The modeled generation time series capture the diurnal cycle and ramp distribution of observed generation reasonably well. The final dataset has a bias of less than 1% and an hourly coefficient of determination (R^2) of 0.89 for the aggregate generation. Figure 4.4 includes the histogram and the frequency duration curve of concurrent, modeled and observed power generation data for the operational wind plants with one year of validation data or more. As shown, the wind profiles capture the dynamic behavior of generation at the operational wind plants.

[4.20] UL did not model the power consumption of hot or cold weather packages as no information was available regarding their installation.

[4.21] The historical generation data is described in Section 4.1.1

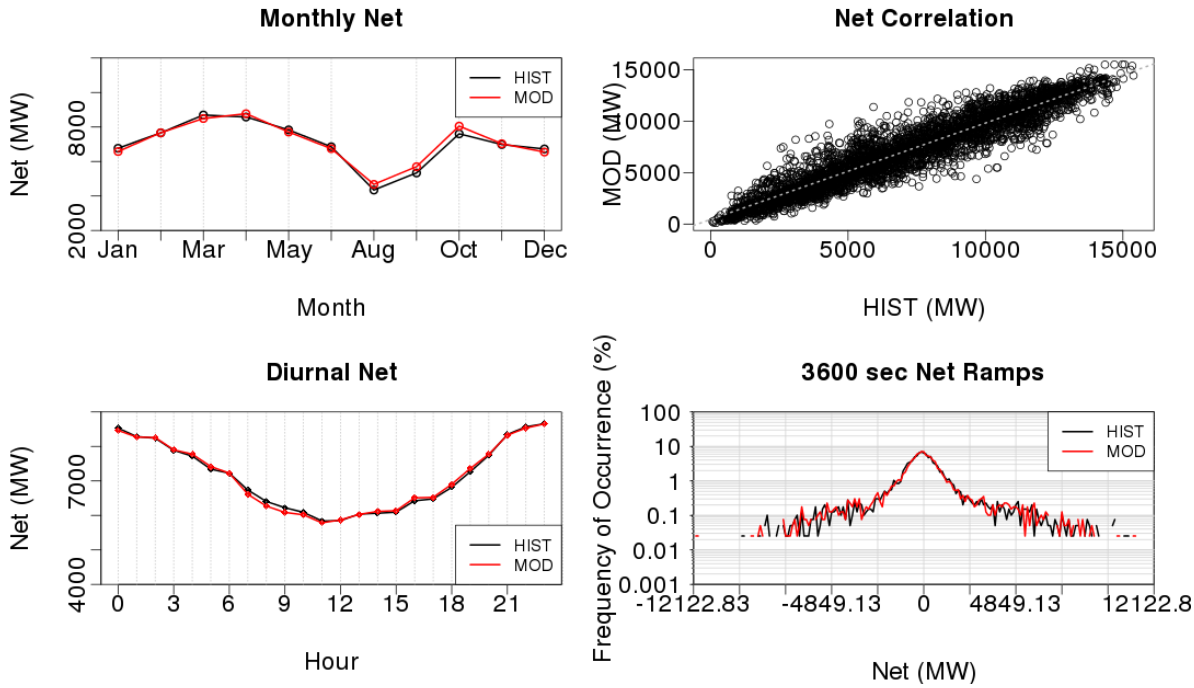

Figure 4.3: Monthly, Hourly and 1-Hour Ramp Distribution of Aggregated Operational Wind Plant Time Series for Concurrent Observed (black) and Modeled (red) Net Power with Correlation Plot (local standard time).

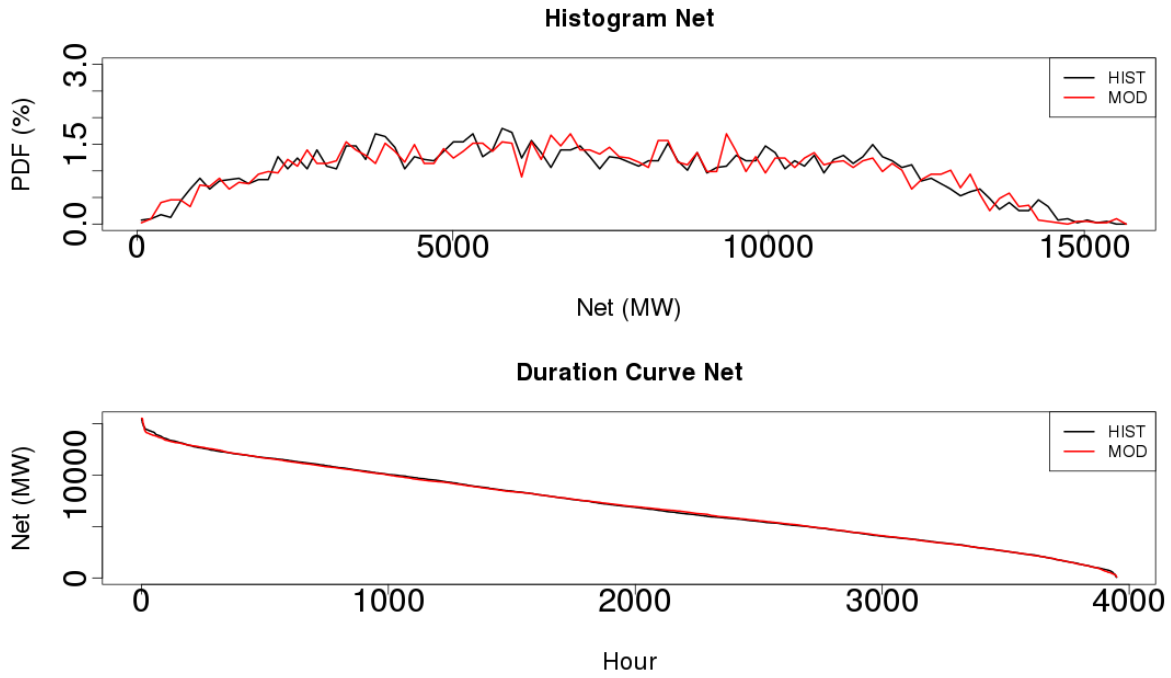

Figure 4.4: Probability Distribution Function and Duration Curve of Aggregate Operational Wind Plant Time Series for Concurrent Observed (black) and Modeled (red) Net Power

4.5 Wind Power Generation Results

Hourly net generation profiles were simulated for the period 1980-2019 across 150 operational plants and 148 hypothetical plants within the ERCOT domain (Figure 4.5). The net capacity factor (NCF) of the modeled generation time series range from 21.1% to 52.1% for the operational plants, and 31.3% to 53.4% for hypothetical plants (Table 4.1).

The power generation across the ERCOT domain shows a peak in the overall generation during the spring months and a lull in late summer; the diurnal pattern exhibits a peak in the generation during the overnight hours (Figure 4.7). However, this pattern does not describe the typical generation at all sites within the domain.

The power generation by CDR zone is shown for operational and hypothetical plants in Figure 4.7 and Figure 4.8. As shown, the pattern of generation in the West CDR zone dominates the overall domain-wide aggregate for both the operational and hypothetical plants, as the West CDR zone has the highest modeled capacity (53% of operational capacity and 31% of hypothetical capacity). Generation is dominated by increased wind speeds during the springtime in part due to relatively high baroclinicity (temperature gradients), which manifests as windy springtime cold fronts. This baroclinicity is diminished as the warm season progresses. Another phenomenon develops at an inland location during the spring and summer as well: the nocturnal low-level jet. Much of the production in the summer in Texas comes from the nocturnal low-level jet, a phenomena during which nighttime cooling produces a shallow stable layer of air and winds just above the surface speed up because of reduced frictional effects. Because of the jet, wind generation peaks in the overnight and early morning hours, with a typical down ramp during the morning load ramp up. Along the coast, a sea breeze circulation is driven by the temperature difference between the land and sea. This circulation drives winds ashore during the daytime heating of the land surface. Hence, winds at hub height near the coast peak during the late afternoon.

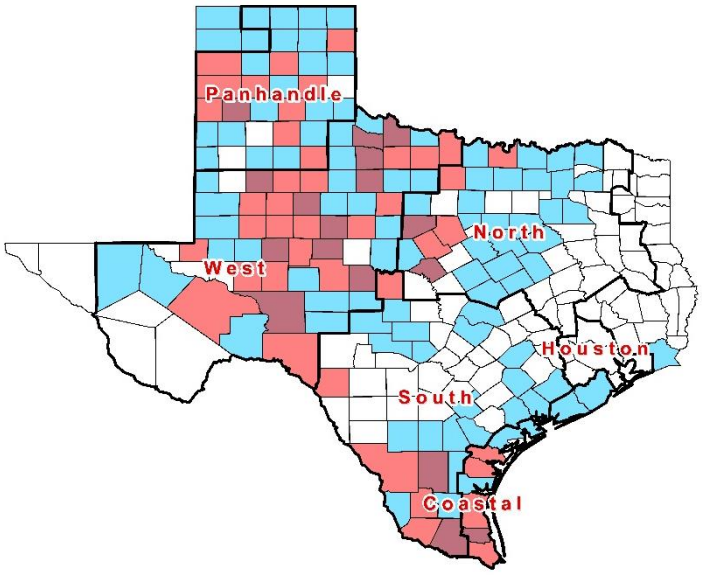

Figure 4.5: Counties Intersecting Hypothetical (blue) or Operational (red) Wind Plants with CDR Zones Outlined

Table 4.1: Generation Summary by CDR Zone for Operational and Hypothetical Wind Plants

Zone	Hypothetical			Operational		
	Cap (GW)	Avg NCF	Range NCF	Cap (GW)	Avg NCF	Range NCF
Coastal	1.6	41.0%	33.9 - 44.8%	3.3	32.5%	24.3 - 37.3%
North	7.1	43.1%	36.9 - 53.2%	1.3	39.1%	29.6 - 46.8%
Panhandle	7.0	47.1%	40.2 - 52.6%	4.4	43.7%	35.7 - 52.1%
South	5.6	40.9%	31.3 - 49.1%	2.3	39.5%	30.6 - 44.8%
West	9.4	47.3%	33.6 - 53.4%	12.6	35.3%	21.1 - 51.5%
Total[4.22]	30.9	44.7%	31.3 - 53.4%	24.0	37.1%	21.1 - 52.1%

[4.22] The totals for the hypothetical plants include two sites that are not within any ERCOT CDR zone: site 730 and site 750 (both in Jefferson county).

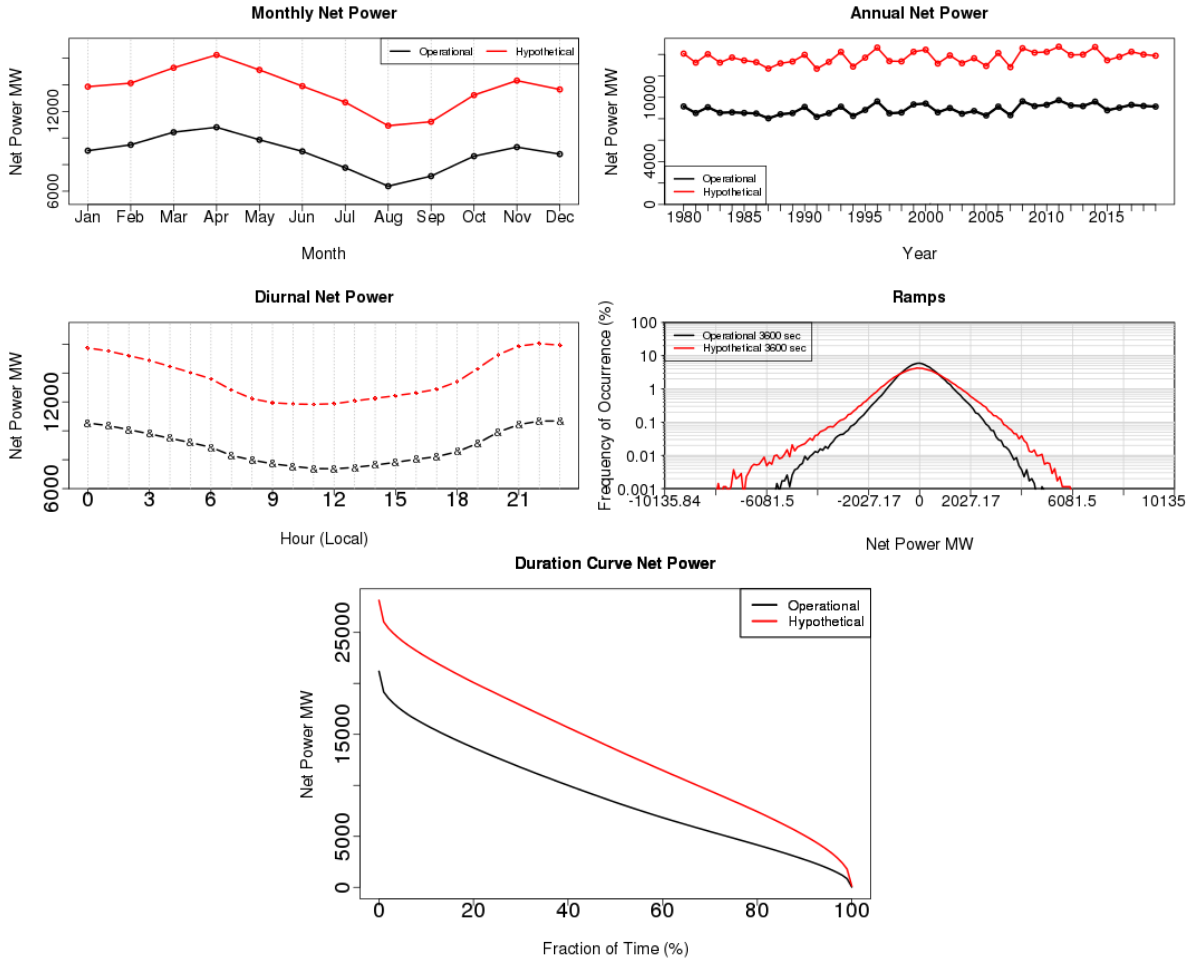

Figure 4.6: Aggregated Monthly, Diurnal, and Annual Net Power, 1-Hour Ramp Distribution, and Duration of Net Power Generation for Modeled Wind Plants (local standard time)

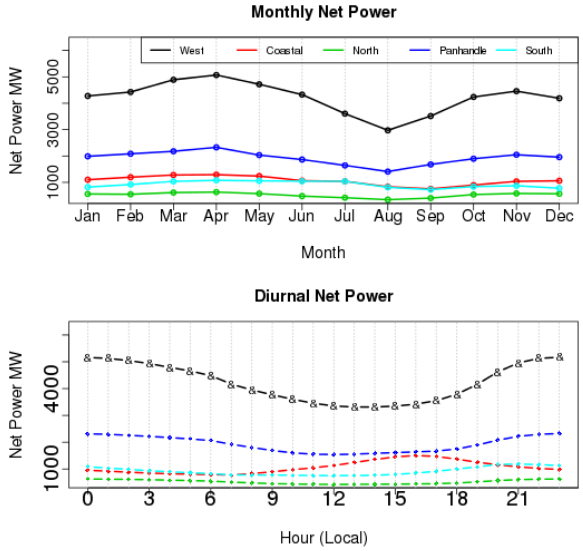

Figure 4.7: Monthly and Diurnal Modeled Net Power for Operational Wind Plants by CDR Zone (local standard time)

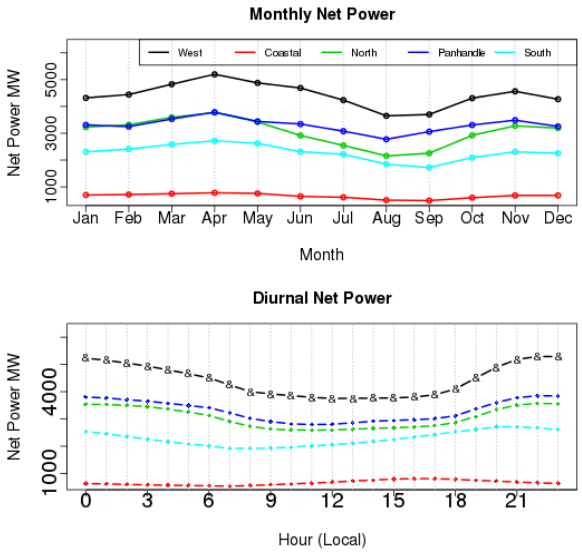

Figure 4.8: Monthly and Diurnal Modeled Net Power for Hypothetical Wind Plants by CDR Zone (local standard time)

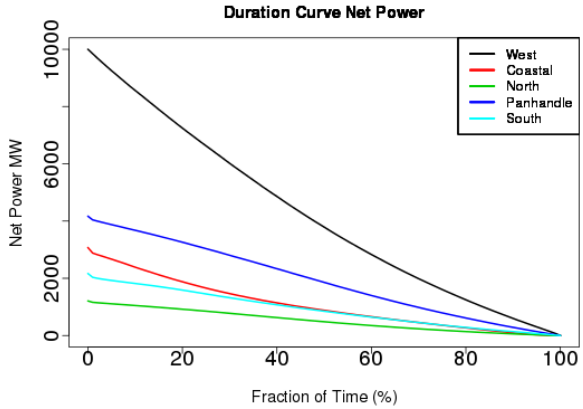

Figure 4.9: Duration of Modeled Net Power Generation for Operational Wind Plants by CDR Zone

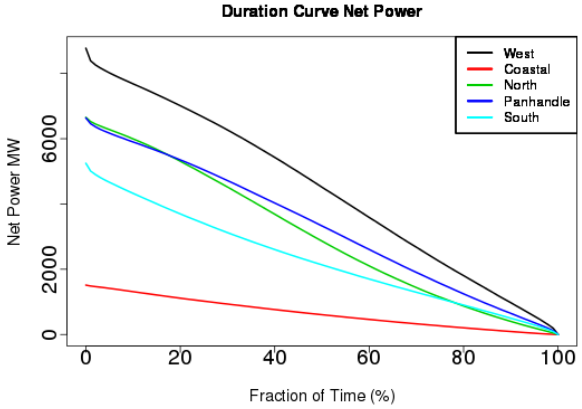

Figure 4.10: Duration of Modeled Net Power Generation for Hypothetical Wind Plants by CDR Zone

5. UTILITY-SCALE SOLAR PLANTS

5.1 Operational and Planned Solar PV Plants

5.1.1 Plant Characteristics

Solar plant details were compiled to best ensure completeness and accuracy of the ERCOT fleet to be modeled. ERCOT provided the centroid coordinates and static plant details of each unit code including installed MW capacity (AC and DC), county, tracking type, and the make and models of the inverter and modules at each plant. A total of 40 individual generating units, as designated by their RARF unit code name, were modeled. Each plant was classified as operational or planned (non-operational) based on the availability of generation data and client-provided information. RARF unit codes were aggregated for multi-phase projects if the phases were geographically aligned such that no obvious distinction could be made between their layouts. Following the review and consolidation process, a total of 35 utility-scale PV plants were modeled, representing all the RARF unit codes provided by ERCOT (Appendix

C). This information was reviewed for consistency and compared to information derived from outside sources.

5.1.2 Operational Plant Data

Observed generation data concurrent with the modeling period was received from ERCOT and subsequently screened for reasonableness. Data from individual plants start on the date that ERCOT approved commercial operations, and therefore did not require truncating for a break-in period. The historical generation data for most plants consisted of the hourly high sustainable limit (HSL) for each record. The HSL refers to the limit established by the plant owner/operator (i.e., qualified scheduling entities) that describes the maximum sustained energy production capability of the plant at that time. In essence, the HSL reflects the expected, uncurtailed power generation at actual plant availability which is monitored in real-time and also available historically for each plant registered with ERCOT as a Generation Resource.[5.23]

The remaining historical generation at each plant was quality controlled as follows. Historical power generation was verified not to exceed the plant capacity. The record-to-record variability was analyzed, verifying that concurrent records of generation were not identical.[5.24] Fluctuations in generation were evaluated to assess any unaccounted for change in capacity or temporal reporting convention (i.e. verifying all generation time series are reported in UTC or local standard time, not a mix of multiple time conventions). Datasets were discarded if they did not pass these quality-control tests, have sufficient period of record, or provide meaningful values for validation and adjustment. Of the 35 utility-scale plants modeled, 21 had greater than 6 months of valid data and 18 had over 24 months. The remaining 14 plants had either less than 6 months of valid data or no data at all. The utility-scale plants modeled were categorized as below based on their operational status, the availability of generation data, and knowledge of static plant details. Two categories emerged:

- operational plants (centroid coordinate specified, PV module(s) and inverter(s) known; generation data sufficient for adjustment tuning to operational data); and
- planned plants (centroid coordinate specified, PV module(s) and inverter(s) known; generation data insufficient or unavailable; composite adjustment from operational tuning).

5.2 Hypothetical Solar PV Plants

UL performed a solar site screening for ERCOT where many new hypothetical utility-scale PV plants were identified to expand the geographic distribution of the sites previously modeled.[5.25, 5.26] In total, 139 hypothetical utility-scale sites were identified, with a single site in each county denoted in Figure 5.1. These sites were selected based on their resource potential and proximity to key operational or planned utility-scale solar PV plants, and distance to transmission. All 139 sites modeled satisfy *at least one* of the following criteria:

- relatively high irradiance resource
- within 25-30 km of operational plants;
- within 3 km of existing transmission of a suitable size for the size capacity;

[5.23] The HSL data is not available for one operating plant; as a Settlement Only Generator (SOG) it is not required to provide HSL data to ERCOT. Historical power generation data, including any plant losses and curtailment was provided.

[5.24] In UL's experience, power generation data that is stuck on a constant value is often indicative of data transmission issues.

[5.25] Rojowsky, K. (2017). Solar Site Screening and Hourly Generation Profiles. Technical report prepared for ERCOT by AWS Truepower. Reference number: 03-16-014484

[5.26] Rojowsky, K. (2019). Utility-scale Solar and Distributed Rooftop Generation Profiles for Select Urban Areas. Technical Report prepared for ERCOT by UL. Reference number 19-02-025140.

- or in a county with planned utility-scale PV sites as of 2019 (per ERCOT GIS reports[5.27]).

Given the above criteria, the 139 final hypothetical plants of 50 MW_{AC} each, totaling 6.95 GW, were modeled.

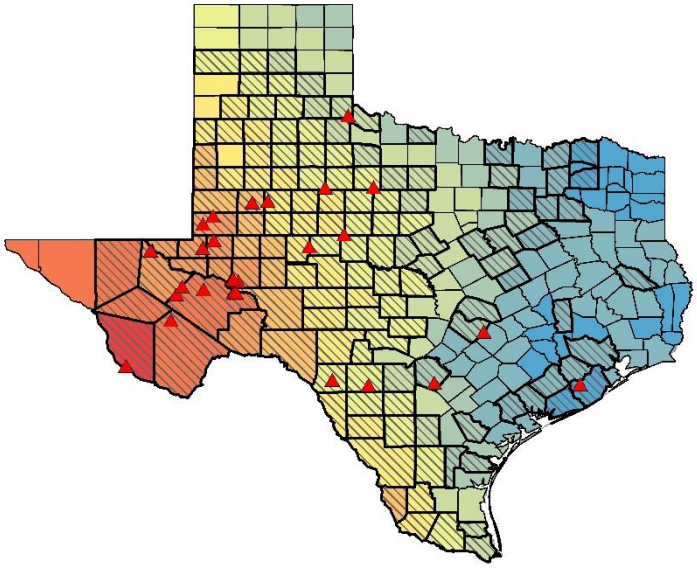

Figure 5.1: Counties with Hypothetical PV Plants (shaded) and Operational or Planned PV Plants (triangles), with GHI Resource as Background

5.2.1 Near-Current Composite Technology

Representative near-current PV technology specifications for hypothetical sites were developed with UL's industry knowledge and survey of technology trends from VDMA (Verband Deutscher Maschinen- und Anlagenbau, German Engineering Federation). Leveraging future technology assumptions developed for previous solar profiles in the ERCOT region, efficiency gains for the utility-scale and rooftop composite modules were updated based on projected technology innovation and trends predicted in VDMA's International Technology Roadmap for Photovoltaics (ITRPV).[5.28] The composite module specifications (Table 5.1) are based on simplified assumptions from the ITRPV. The near-current module technology only accounts for crystalline modules; thin film and bifacial technology are not represented. The efficiency specifications assume the market share in 2025 will primarily consist of aluminum Back Surface Field (Al-BSF) and Passivated Emitter and Rear Cell (PERC) modules.

Both utility-scale and rooftop composites had their specifications updated most notably by an increase in the energy density (W/m^2) derived from the module rated capacity (W) and area (m^2). In general, the trend is for higher wattage and more efficient panels, with reduced temperature losses. For rooftop installations, 72-cell and higher wattage modules are being favored due to space constraints and affordable pricing.

The increase in module rated capacity and energy density has some notable implications for the modeled PV plants and distributed rooftop areas. For hypothetical operational plants modeled at 50

[5.27] ERCOT. Monthly Generator Interconnection Status Report. Available at http://www.ercot.com/gridinfo/resource

[5.28] International Technology Roadmap for Photovoltaics (ITRPV) 9th edition. Verband Deutscher Maschinen- und Anlagenbau, German Engineering Federation, 2018 (http://www.itrpv.net)

MW, the footprint required to build out such an installation is now smaller than implied in previous work. For rooftop, regional capacity estimates were developed by applying energy density estimates to the total area of suitable land. Therefore, an increase in the energy density (W/m^2) of modules directly increases in future capacity estimates (Section 6).

Table 5.1: Module Specifications for Near-Current Technology

Module	Rated Capacity (W)	Efficiency (%)	Temperature Coefficient of Power (%)	Area (m^2)
Utility (2019)	325	18.9	-0.41	1.94
Rooftop (2019)	261	18.4	-0.42	1.63
Utility (2020)	350	19.2	-0.37	1.94
Rooftop (2020)	375	18.7	-0.37	1.94

6. DISTRIBUTED SOLAR GENERATION SITES

6.1 Simulated Rooftop Generation for Greater Metro Areas

The greater metro areas of Austin, Dallas, Houston, and San Antonio were evaluated for potential distributed rooftop generation PV (DGPV) by estimating the rooftop area available for solar panels. A total of 12 DGPV aggregate sites were identified within these four metro regions, and each was defined according to their intensity of development (high, medium, or low). In 2020, land use and land class information within the metro boundary was updated,[6.29] and more detailed road exclusions were applied.[6.30] The energy density per unit land area was then approximated using aerial imagery and reasonable development assumptions for each land class (Table 6.1).[6.31] The resulting energy density assumptions were applied to the available land area to obtain the potential DGPV capacity for each metro area (Table 6.2). These capacities were used to model the DGPV profiles for the 12 aggregate sites in this study. The total metro area rooftop capacity increased from 18.4 GW in 2019, to 24.1 GW in the present study.

Table 6.1: Distributed PV Assumptions by Intensity of Development

2020	Low	Med	High
Buildings (% of land area)	20	26	35
Optimal (% of buildings)	50	50	90
Usable (% of optimal)	18.75	18.75	60
Plant density assumption (W/m2)	55	55	65
Final density assumption (MW/km2)	1.03	1.34	12.29
2017	**Low**	**Med**	**High**
Final density assumption (MW/km^2)	0.84	1.10	9.45

[6.29] National Land Cover Database 2016 (NLCD 2016). Multi-Resolution Land Characteristics Consortium. http://www.mrlc.gov/

[6.30] U.S. Census Bureau's 2014 TIGER database map image layer for ArcGIS. Esri. Available at https://landscape1.arcgis.com/arcgis/rest/services/USA_Roads/MapServer

[6.31] These energy density assumptions have been updated to reflect the near-current composite technology used for power conversion in the current study.

Table 6.2: Capacity (MW_{AC}) by Metro Area and Intensity of Development

Metro Area	Low	Medium	High	Total
Austin	374	411	1,405	2,190
Dallas	1,557	1,611	6,552	9,720
Houston	1,211	1,779	6,677	9,667
San Antonio	420	431	1,672	2,523
Total (GW)				*24.1*

6.2 Simulated Rooftop Generation for Rural Regions

In 2020, UL worked with ERCOT to develop a methodology to estimate the potential distributed rooftop PV generation across rural counties within ERCOT. Regional distributed generation profiles, excluding areas already represented by the greater metro regions of Austin, Dallas, Houston, and San Antonio, were characterized using GIS information as follows.

A database of city limit boundaries from the Texas Department of Transportation (TxDOT) was used to identify population centers that exceeded a minimum threshold to be further screened for profile development.[6.32] Land use data within these populated areas was used to delineate the modeling areas.[6.25] PV profiles were modeled for areas comprising of low, medium, and high intensity development within the TxDOT database, not including the four greater metro regions previously described. These locations are collectively referred to as the "rural development areas". Of the 231 counties in ERCOT, 221 counties had rural development areas identified for PV profile modeling (grey counties in Figure 6.1). The appropriate energy density assumptions (MW/km^2) were applied to the corresponding land area totals within each land use class to obtain the potential DGPV capacity for each rural development area. The potential capacity of rural development areas is provided by CDR zone in Table 6.3. The final modeled profiles provided are aggregates of rural area DGPV generation within each CDR zone.

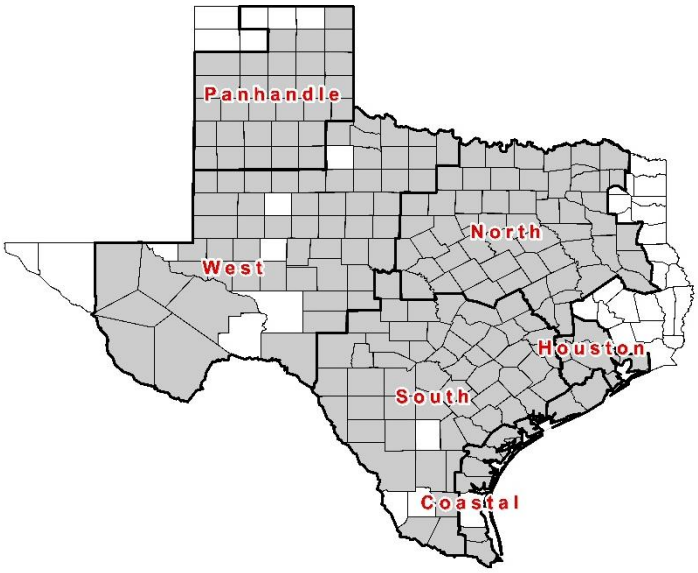

Figure 6.1: Counties Represented by Rural Profiles

[6.32] TxDOT City Boundaries feature layer for ArcGIS. Esri. Available at http://gis-txdot.opendata.arcgis.com/datasets/txdot-city-boundaries

Table 6.3: Rural Distributed PV Capacity by CDR Zone

Zone	Cap (MW_{AC})
Coastal	835.98
Houston	249.32
North	1965.63
Panhandle	564.31
South	1497.02
West	863.70
Total	*5975.96*

7. SOLAR GENERATION PROFILES

7.1 Solar Power Generation

UL simulated hourly generation using the adjusted WRF modeled time series at the utility-scale and DGPV rooftop sites. Atmospheric variables that impact module performance and power conversion were extracted from the WRF numerical data output and the modeled irradiance was converted to solar PV output using UL's power conversion software, TS2Solar Version 4.2.0. Operational sites were modeled with plant-specific parameters as agreed upon by ERCOT and UL. Hypothetical sites were modeled with the generic site characteristics listed in Table 7.1 and the near-current composite modules described in Section 5.2.1. All hypothetical utility-scale systems were assumed to be facing south and single-axis sites were assumed to be tilted horizontally.[7.33] DGPV systems were assumed to be tilted to 22.6 degrees (a common rooftop pitch in Texas) and were modeled using a variety of azimuths to capture real-world scenarios in which roofs may not be optimally oriented.

Table 7.1: Static Plant Details for Hypothetical and Distributed PV Sites

Plant Type	Tracking System	Tracking Type	Tilt (°)	Azimuth(s) (° from S)	DC:AC ratio
Utility	Single	N-S	0	0	1.30
Utility	Dual	NA	NA	0	1.25
Aggregate DGPV	Fixed	NA	22.6	+/-45, 0	1.25

The power conversion process follows the methodology in AWST (2017). However, the current software version has improved accounting of time-varying temperature-related losses. Details of the power conversion can be found in AWST 2017,[5.2. 5.23] and a listing of static loss assumptions are in Table 7.2.

[7.33] This differs from AWST (2017), where single-axis hypothetical plant panels were assumed to be tilted to the mean latitude of the site.

Table 7.2: Static PV Loss Assumptions

Loss Source	%
Non-STC Operation (Irradiance)	0.50
Initial Light-Induced Degradation (Crystalline, Thin Film)	1.50, 2.00
Module Quality (Crystalline, Thin Film)	1.00, -1.00
Module Mismatch	1.25
Inverter Efficiency	1.50
DC wiring	0.80
Tracking System Performance (if applicable)	0.20
Availability of System and Substation	0.80
HVAC and Auxiliary Components	0.00
Yearly Module Degradation	0
AC wiring	0.80
Transformers	1.75
Transmission	0.00

7.2 Adjustment and Validation

The modeled solar generation data were adjusted using quality-controlled, hourly-ending historical generation data to more accurately reflect real-world power generation patterns. The main purpose of this adjustment is to account for discrepancies in static plant details (e.g., layout, equipment, tilt, tracking characteristics), loss assumptions, and any other deficiencies in the modeling process. The final adjustment process applied a two-dimensional correction matrix specific based on concurrent observed and modeled power generation at every month and hour.

7.2.1 Utility-Scale Solar PV

Historical generation data from operational utility-scale plants were used to adjust the modeled profiles at all utility-scale PV plants (operational or planned, and hypothetical). For operational plants with greater than 6 months of valid data, the modeled data for each respective plant were used in a custom adjustment. A composite adjustment developed from all operational plants with valid historical data was used to adjust the hypothetical plant profiles and the profiles of the operational or planned utility-scale solar plants that did not have sufficient generation data for custom adjustment (less than 6 months of valid data).[7.34]

After adjustment to monthly and diurnal expected values, the overall generation time series were scaled to the observed maximum value at each plant. Therefore, modeled generation will reach 100% of the nameplate MWAC capacity at the operational sites if the historical data reaches 100% capacity. For hypothetical sites, the modeled generation reaches 100% of the MWAC capacity (50 MWAC).

The final generation profiles were examined for reasonableness at the plant level and as an aggregate for the operational plants with at least one year of available historical generation data. The adjusted modeled generation time series match the observed monthly and diurnal patterns (as expected with an adjustment based on month and hour) and also captures the observed hourly ramp frequency distribution well (Figure 7.1). The final dataset has a bias of 0.0% on generation and an hourly coefficient

[7.34] The use of operational data to adjust the hypothetical profiles assumes that the hypothetical sites will operate like the existing operational sites, including availability issues inherent in the observed generation data. Also, deficiencies in the static plant details of operational plants and subsequent modeling process will be reflected in this adjustment. Therefore, the adjusted profiles may represent a conservative lower bound for the generation at future hypothetical sites given historical availability patterns and the static assumptions provided for the operational sites. High-quality operational plant metadata (static data) may benefit future work when adjusting to operational data.

of determination (R^2) of 0.92. Depicted in Figure 7.2 is the frequency duration curve for all concurrent, hourly historical and adjusted model data for plants that had at least one year of historical generation data. This analysis shows that the final dataset accurately captures the dynamic behavior of utility-scale solar plants.

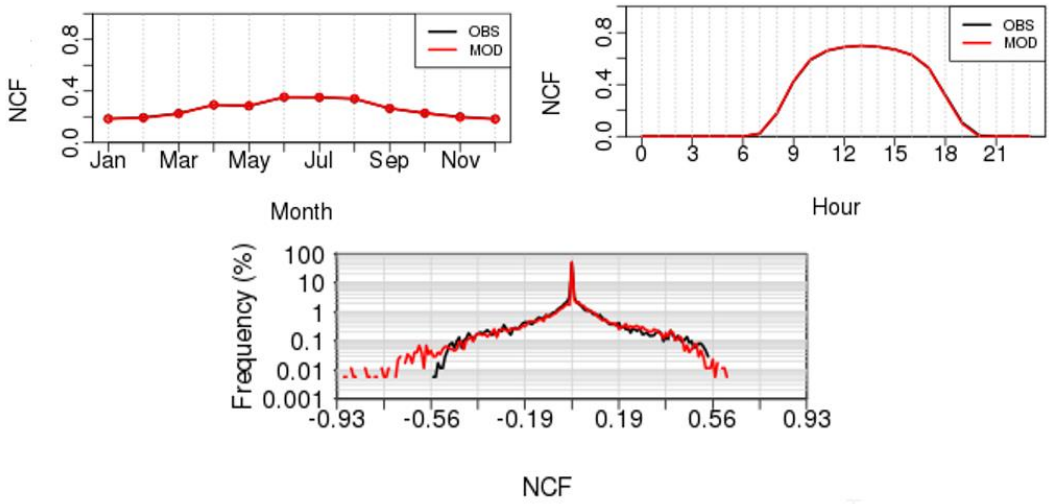

Figure 7.1: Hourly Mean Monthly (top left), Diurnal (top right) and Ramp Frequency Distribution (bottom) NCF for an Aggregate of Operational Solar Plants (local standard time)

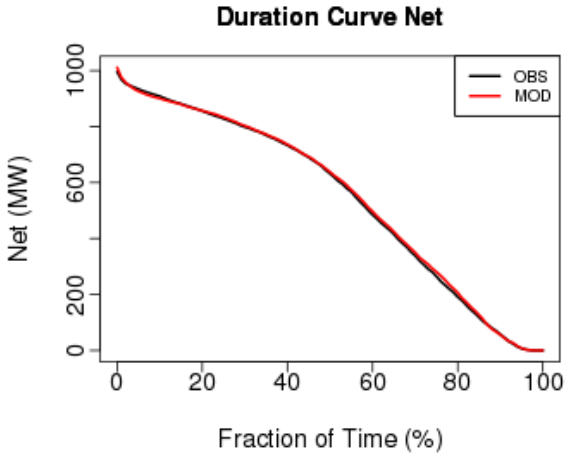

Figure 7.2: Frequency Duration Curve for Operational Solar Plants

7.2.2 Distributed Rooftop Sites

For the distributed rooftop generation profiles, a composite matrix was developed using 2019 historical rooftop generation data from zip codes in each of the metro areas. All DGPV metro areas and rural sites were adjusted using this matrix. The resulting modeled profiles were scaled to the maximum observed over the period; therefore, DGPV metro and rural profiles reach 97.5% of the assumed MW_{AC} capacity.

The final generation profiles were examined for reasonableness at the site level and as an aggregate of all the zip codes for which rooftop generation data was obtained (Figure 7.3). As with the modeled utility-scale generation time series, these modeled DGPV generation time series accurately depict the

diurnal and monthly mean patterns of observed generation data. The model overestimates the largest ramps, which provides a conservative estimate of the hourly ramping potential of DGPV across these metro areas. The final dataset has a bias of -1.1% on generation and an hourly coefficient of determination (R^2) of 0.94. Depicted in Figure 7.4 is the frequency duration curve for all concurrent, hourly historical and adjusted model data for generation data across the four metro areas. This analysis shows that final dataset accurately captures the dynamic behavior of distributed rooftop generation.

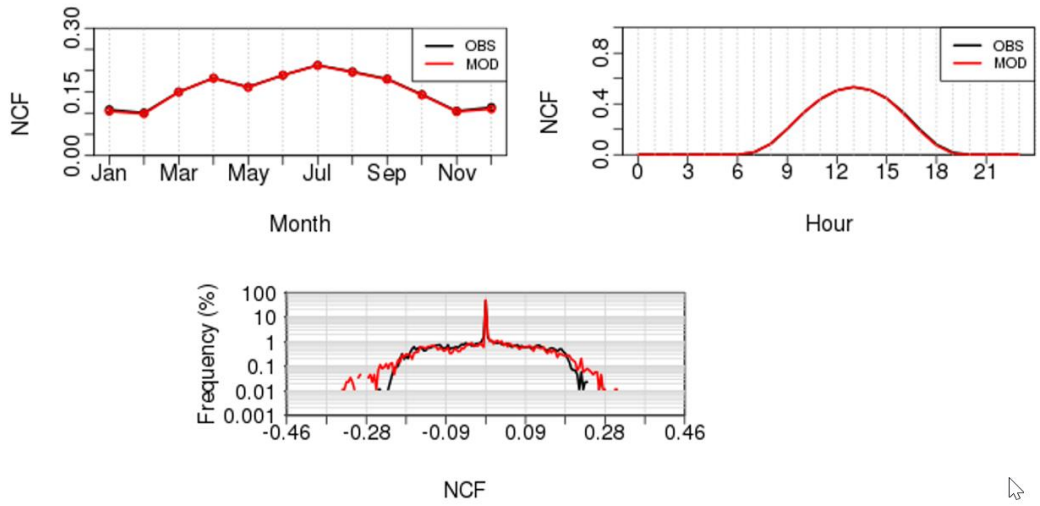

Figure 7.3: Hourly Mean Monthly (top left), Diurnal (top right) and Ramp Frequency for Aggregated Rooftop Data (local standard time)

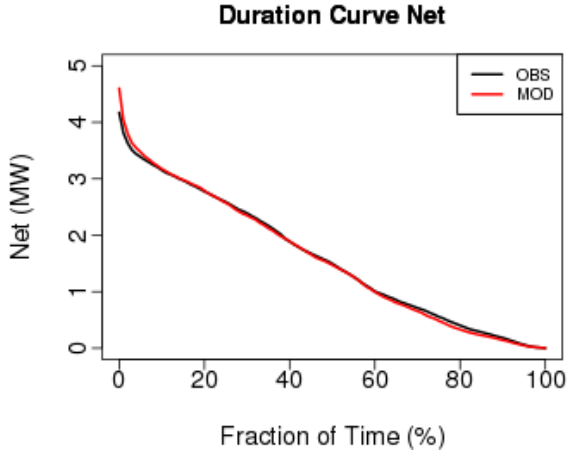

Figure 7.4: Frequency Duration Curve for Aggregated Rooftop Data

7.3 Solar Power Generation Results

Hour-ending time series of PV generation profiles were developed for 139 hypothetical utility-scale sites, 35 operational or planned utility-scale plants, 12 DGPV sites across four metro areas, and six CDR zone DGPV rural profiles for the years 1980-2019 (Figure 7.5).

The range of net capacity factors (NCF) for each site type can be found in Table 7.3. The operational plants have mean NCFs ranging from 18.7% to 31.0%. Note that two of these plants (Sites 5 and 24) had lower than expected historical generation based on the local irradiance resource, which is reflected in their modeled profiles after tuning to this data. As expected, the hypothetical plant profiles modeled

with near-current technology show higher values of min and max NCF than the operational, with double-axis tracking generation higher than single-axis tracking (Appendix D). The use of operational data to adjust the hypothetical profiles assumes that the hypothetical sites would operate like the existing operational sites (i.e., with equivalent availability). Generally, the DGPV profiles exhibit the lower NCFs than the utility-scale PV plants. Even when accounting for local irradiance resource, generation varies between centralized, utility-scale and distributed rooftop generation due to plant characteristics. These differences are largely due to: tracking (fixed rooftop PV compared vs. tracking utility-scale systems); module technology; and modeling assumptions (rooftop systems were assumed to have wind-driven cooling only on one face of the panels and thus experienced higher temperature losses).

The monthly and diurnal mean net power at a sample hypothetical site is shown in Figure 7.6. As expected, the dual-axis profiles exhibit higher power than the single-axis counterparts during midday and in the winter, when dual-axis trackers are better able to maximize production during the sun's low wintertime altitude compared to the single-axis trackers, which are flat midday.[7.35] This difference is more pronounced with increasing latitude (not shown).

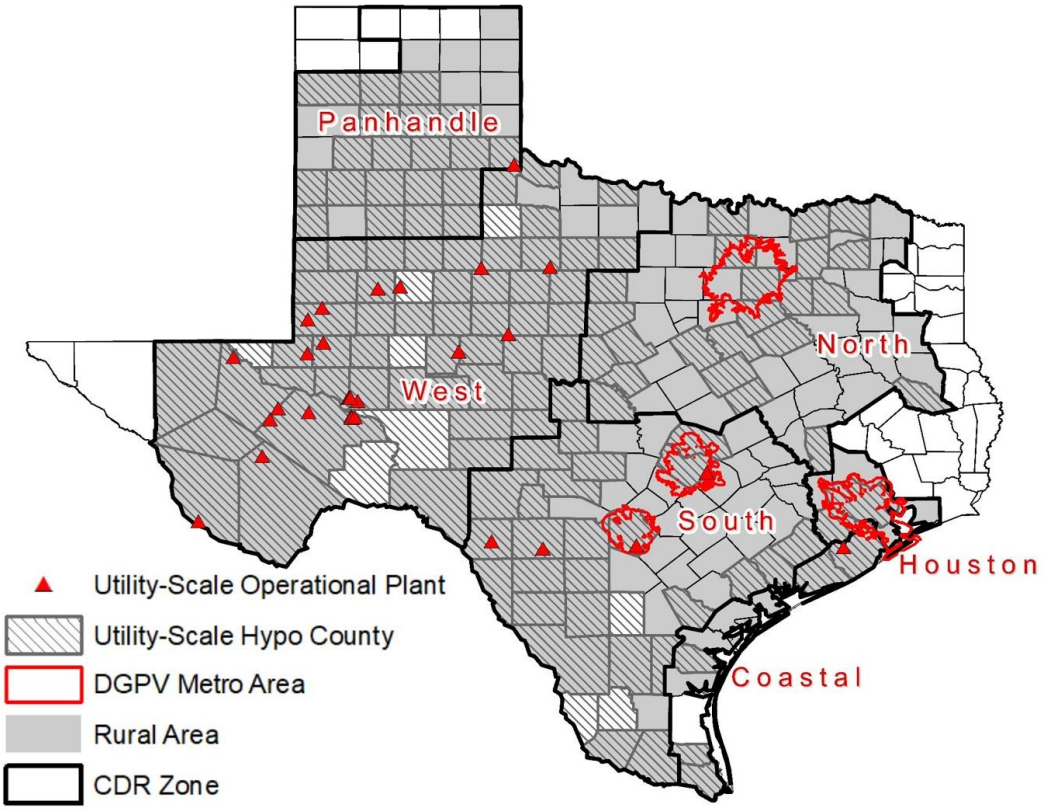

Figure 7.5: Areas Represented by Modeled PV Profiles

[7.35] The final generation profiles for the dual-axis trackers exhibit slightly lower NCF during the summertime than their single-axis counterparts, primarily due to the adjustment to observed generation data where this is seen.

Table 7.3: Range of Net Capacity Factors (NCFs) for Modeled Solar PV Time Series

PV Generator Type	Range NCF (%)
Operational and Planned Utility-Scale	18.7 – 31.0
Utility-Scale Hypothetical (Single-Axis)	22.7 – 31.9
Utility-Scale Hypothetical (Dual-Axis)	23.4 – 32.4
Distributed Rooftop (Metro)	14.9 – 15.4
Distributed Rooftop (Rural)	14.5 – 20.4

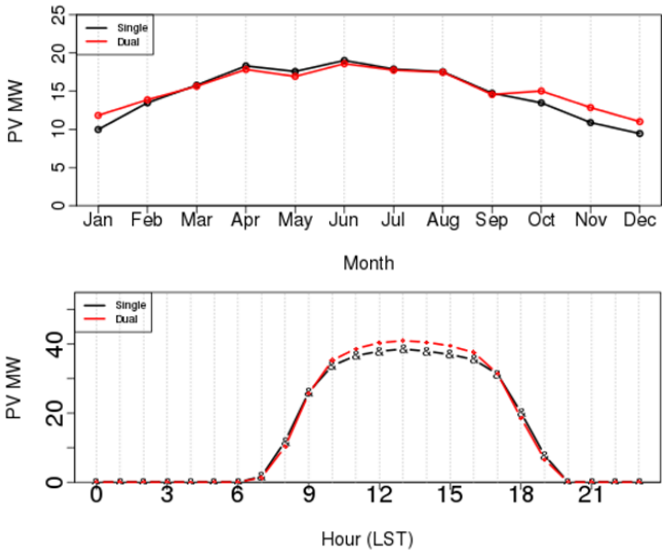

Figure 7.6: Monthly and Diurnal Mean Net Power at a Sample Hypothetical Site modeled as Single-axis (black) and Dual-axis (red) Tracking (local standard time)

The distributed rooftop generation profiles were evaluated for differences in the potential generation across the metro areas. As seen in previous work, the overall net capacity factor varies little across the different land use classes within individual metro areas, but the normalized generation does vary across the four metro areas, due to differences in local climates. Further analysis also shows a difference in the timing of generation across these four metro areas, as shown by the average diurnal NCF calculated as a sum of all three land class sites per metro area (Figure 7.7). All profiles achieve non-zero generation at the same hours (06:00 and 19:00) and peak generation at the same hour (13:00). However, the effect of longitude on the relative solar position can be seen in the mean diurnal NCF, with Houston power generation reaching higher generation earlier in the morning, followed by Dallas, Austin, and San Antonio, from east to west. The opposite pattern, although less well pronounced, is seen in the afternoon. The influence of increased cloudiness in eastern Texas is seen in the lower NCF in Houston, particularly in the afternoon.

The diurnal profile of distributed rooftop PV generation was compared to neighboring utility-scale hypothetical sites. The diurnal profile for Austin DGPV metro area and an intersecting hypothetical site is shown in Figure 7.8. The overall peak amplitude and shape of the diurnal profile varies substantially between distributed rooftop PV generation profiles and the neighboring utility-scale site, for the reasons discussed above.

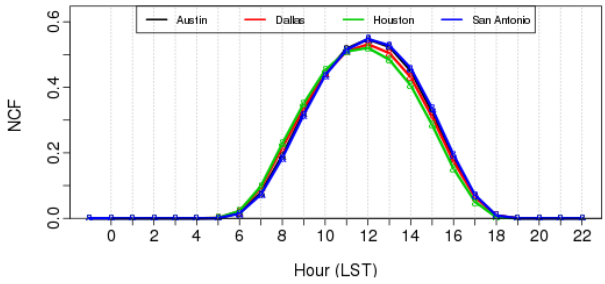

Figure 7.7: Diurnal Net Capacity Factor for DGPV metro areas

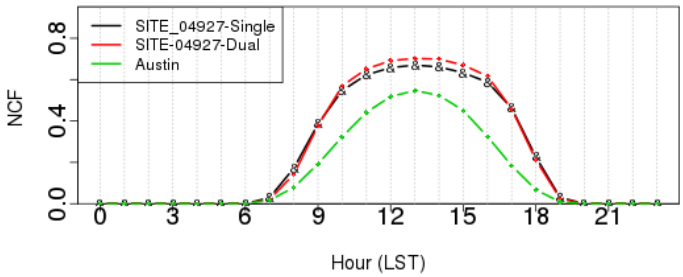

Figure 7.8: Comparison of NCF for Aggregated DGPV Austin Metro Area and an Intersecting Hypothetical Site (local standard time)

Similar to the DGPV metro profiles, analysis of the DGPV rural profiles show a difference in the timing of generation across the CDR zones, as shown by the average diurnal NCF profile calculated for each zone (Figure 7.9). All profiles achieve non-zero generation at the same hours (06:00 and 19:00) and peak generation at the same hour (13:00). Similar to the DGPV metro profiles, the Coastal, North, and Houston power generation reach a higher generation earlier in the morning followed by South, West, and Panhandle from east to west. The opposite pattern is seen in the afternoon. The influence of increased cloudiness in eastern Texas is seen in the lower NCF in Houston, particularly in the afternoon.

The seasonal variation in distributed solar generation is also shown by CDR zone in Figure 7.10. The aggregate generation shows the most disparity between CDR zones (Appendix E) during the late fall through spring, and the most uniform generation potential during the summer months and into the early fall. The typical weather pattern in Texas features westerly (dry) winds off of the Rockies and the high plateau of northern Mexico meeting southerly and southeasterly (moist) winds from the Gulf. During most of the year, this creates large-scale instability and relatively frequent cloudiness in eastern Texas (with clouds diminishing to the west). From late fall and throughout winter, strong ridging along the west coast of the U.S. frequently leads to a broad upper-level trough pattern over the central U.S. Because of this, cold air moves south down the Great Plains and low pressure frequently develops over central and eastern Texas. This setup can last for days and repeat several times in a month, engulfing northern and eastern parts of the state with cloudiness. These upper level features relax during the summer, creating for much weaker and more “zonal” flow aloft. Strong high pressure is typically found over the region in summer and early fall, bringing sunny and quiescent conditions across the region in the heat of the warm months.

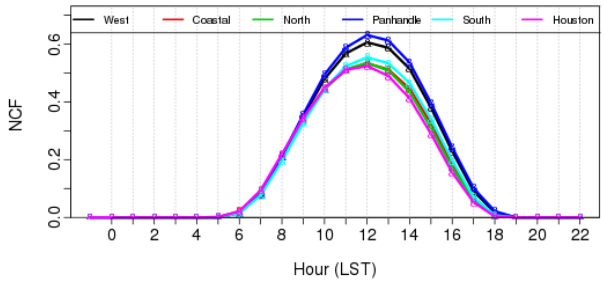

Figure 7.9: Diurnal Net Capacity Factor for DGPV Rural Zones (local standard time)

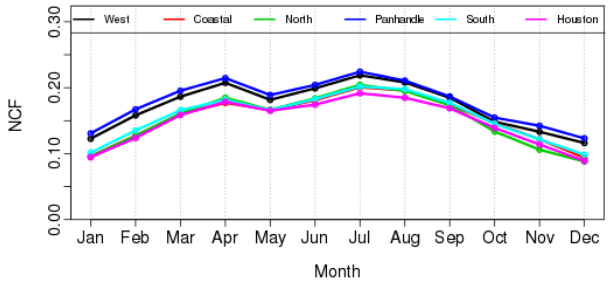

Figure 7.10: Monthly Net Capacity Factor for DGPV Rural Zones (local standard time)

8. DATASET USAGE

The goal of this work was to provide high fidelity power generation profiles for operational and hypothetical installations to support regional planning studies. Therefore, it is important to understand the modeling assumptions and methods applied to guide their future use and application.

UL simulated ERCOT's wind power profiles using Openwind, a state-of-the-art resource assessment, and power optimization modeling tool used across the wind industry during all phases of project development. Openwind calculates plant-level and turbine level losses at each time step including wake, availability, environmental, turbine performance, and electrical losses. Plant-specific characteristics such as plant layout, turbine model, and power curve heavily influence the power generation and wind plant losses on various time scales.

UL adapted the Openwind software allowing for fleet modeling with a high degree of success across large project areas where plant specifications are well documented and supplied as input for modeling. These characteristics were defined for ERCOT's operational wind plants to the best of UL's ability through public and proprietary sources of information. However, in the absence of measured plant-specific losses for this work, UL applied assumptions in the Openwind model based on UL's methods derived from operational plants across North America. These wind profiles reflect a significant change in the methods previously used to simulate wind power profiles in ERCOT, and therefore a record-to-record comparison with previous work may not be appropriate.

It is important to note that simulated wind profiles may not match historical plant generation at a given time for several reasons:

- All plants were modeled for the period 1980-2019 using either the 2017 plant specifications (for previously modeled plants) or the 2019 fleet configuration (for new plants), regardless of the actual commissioning date or any change in plant specifications over time. Information regarding changes in plant configuration or the repowering of operational plants either via a physical change to plant layout or modification to operational turbine settings, power curve etc., were not available.

- Validation and adjustment of wind profiles from previously modeled sites with >1 year of operational data relied heavily on operational data. Wind plants with <1 year of operational data were adjusted using a composite adjustment developed from those with sufficient data.
- The modeled wind data were scaled to historical generation to account for site-specific losses not captured in the model output. The scaling required indicates that input data for the plants may be lacking (e.g. a derating of power curves), or that atmospheric variables contain a bias that affects the Openwind simulation of time-varying losses.
- An attempt was made to remove the effects of grid curtailment from the historical generation data by using the HSL data for the model adjustment. Therefore, the modeled data are not reflective of curtailment that may have been experienced at a wind plant and is present in the actual generation measurements.
- UL did not have an hourly historical record of the actual turbine availability indicating downtime due to events such as preventive or unscheduled maintenance, and plant or grid outages. Instead, the turbine availability was modeled in Openwind with a Markov Chain to best represent the statistical behavior of turbine availability based on a large number of operational plants in the US. Because plant or turbine-level availability was not explicitly given for any plant, it is possible that the modeled availability does not align with the actual availability at each operational plant.
- Some of the operational wind plants modeled for this effort did not have one year of valid data for the final adjustment process (8 of 150 plants). Therefore, an alternative method for modeled data adjustment were developed that may not reflect plant performance at these locations. It is highly recommended that these sites be re-adjusted when a year or more of actual plant generation data is available.

The hypothetical PV sites modeled in this study were identified via a high-level identification of allowable land remaining after exclusions and additional assumptions were applied. A detailed analysis below 200-m resolution was not performed, and therefore some sites may not be commercially viable. Factors such as the total area of contiguous land available to build, construct, and operate a solar PV plant with a reasonable cost of energy have not been considered, neither have policy or regulatory constraints.

Distributed generation rooftop PV (DGPV) is rapidly expanding and while its penetration varies across the landscape, it is highly correlated to land use and population; the drivers used to define DGPV sites for ERCOT in both the metro and rural areas. While the location and potential capacity of DGPV in metro and rural can be assessed assuming current development, future land use changes may affect the location, capacity, and/or modeled characteristics of rooftop installations (e.g., transition of single family homes to multi-unit buildings, commercial real estate development, or an expansion of suburban development). The rooftop PV capacity modeled in this study assumes static land use characteristics in NLCD (2016). Additionally, the distributed solar generation profiles assume all modeled capacity consists of future installations deployed with near-current technology. These profiles do not account for aged technology in-place at existing rooftop installations.

The wind and solar resource were modeled at a 9-km horizontal resolution. While this resolution captures much of the spatial variability in wind and solar resource across the state of Texas, assumptions need to be made about details in the weather patterns. For example, a mesoscale model such as WRF with grid spacing coarser than 4 or 5 km cannot explicitly resolve cumulus clouds, and thus it must rely on convective parameterization scheme. Rather than physically simulating the lifecycle of individual cloud elements, these parameterizations characterize the bulk effects of various cloud types and their lifecycles based on the environmental conditions present at the grid-cell level. Because of this parameterization, the 9-km resolution is generally considered sufficient for hourly solar

generation studies by striking a balance between computational time and the need to resolve localized terrain and roughness effects. For both wind and solar power generation studies, accurate environmental resource characterization is fundamental to replicating real-world power generation. UL incorporated observed wind speed and solar radiation data to ground-truth these specific parameters. However, a bias in any ancillary variables such as temperature, turbulence intensity, relative humidity, or precipitation can adversely affect the modeled wind or solar generation.

This dataset was developed specifically for use in modeling and analysis efforts related to the high penetration of wind and solar and its long-term variability. It has been shown that the final modeled dataset accurately represents the historical generation patterns at individual plants and on an aggregate basis. Additional bias correction for atmospheric variables and updated plant specifications may improve the alignment with the operational data, reducing the need for manual adjustment in the future. Finally, it should be noted that modeled data provided by this study is not a replacement for onsite measurements.

APPENDIX A – OPERATIONAL WIND PLANTS

Table A.1: Operational Wind Plants in Counties A - Fl

SITE #	County	Modeled Capacity (MW)	Data Review
5	Archer	150	
133	Archer	225	
140	Archer	67.62	
45	Baylor	150	
3006	Baylor	30.24	< 1yr
11	Borden	61	
18	Borden	180	
102	Borden	84	
118	Borden	211.22	
12	Briscoe	149.85	
20	Cameron	165	
109	Cameron	95.4	
99	Carson	218.3	
100	Carson	190.79	
46	Carson	200.48	
47	Carson	211.2	
104	Carson	150	
55	Castro	299.7	
114	Clay	204.1	
43	Coke	69.6	
44	Coke	80	
68	Comanche	210.11	
25	Concho	148.35	
135	Cooke	125.6	
139	Cooke	112.5	
122	Crockett	80.25	
82	Dawson	211.22	
56	Deaf Smith	99.9	
57	Deaf Smith	100	
87	Dickens	150	
107	Donley	174	
2014	Erath	100.6	
40	Erath	60	
27	Floyd	50.4	
69	Floyd	200	
28	Floyd	151.2	
115	Floyd	200	
116	Floyd	300.3	
137	Floyd	257.26	

Table A.2: Operational Wind Plants in Counties Fl - No

SITE #	County	Modeled Capacity (MW)	Data Review
138	Floyd	59.8	
3001	Foard	350.28	< 1yr
88	Glasscock	196.6	
94	Glasscock	142.5	
95	Glasscock	115.5	
2105	Glasscock	207.25	
81	Glasscock	90	
54	Haskell	230	
108	Haskell	250	
83	Hemphill	288.6	
84	Hidalgo	150	
85	Hidalgo	100	
2112	Howard	34.32	
34	Howard	121.9	
48	Howard	119.93	
91	Howard	58.8	
13	Jack	120	
61	Jack	110	
111	Jack	150	
36	Jim Hogg	78	
3	Kenedy	202	
130	Kenedy	283.2	
97	Kenedy	403.2	
3007	Kenedy	201	< 1yr
86	Kent	30	
1	Kinney	99.825	
136	Knox	150	
117	Lynn	164.68	
3008	Lynn	300	< 1yr
123	Martin	120	
106	McCulloch	160	
42	Mills	200	
2049	Mills	148.6	
73	Mitchell	49.5	
72	Mitchell	100.5	
131	Mitchell	209	
16	Nolan	232.5	
17	Nolan	170.2	
52	Nolan	223.5	
26	Nolan	126.5	

Table A.3: Oprational Wind Plants in Counties No - St

SITE #	County	Modeled Capacity (MW)	Data Review
59	Nolan	197	
121	Nolan	101.2	
124	Nolan	98.8	
125	Nolan	135	
126	Nolan	135	
127	Nolan	105.8	
128	Nolan	80.5	
129	Nolan	37.5	
132	Nolan	150	
134	Nolan	169.5	
110	Nueces	249	
3000	Oldham	210.105	< 1yr
120	Oldham	160.95	
119	Oldham	194	
79	Parmer	230.4	
60	Pecos	170.25	
92	Pecos	82.5	
62	Pecos	150	
63	Pecos	145	
142	Pecos	82.5	
141	Pecos	77.22	
2	Randall	163.2	
53	Reagan	300	
3002	San Patricio	307.06	< 1yr
3004	San Patricio	162.855	< 1yr
93	San Patricio	179.85	
29	San Patricio	200.1	
32	Scurry	253	
10	Scurry	99	
30	Scurry	130.5	
31	Scurry	120	
41	Scurry	155.4	
101	Scurry	249	
35	Scurry	63	
58	Shackelford	165.6	
71	Shackelford	200	
2070	Shackelford	200	
76	Starr	200	
77	Starr	200	
78	Starr	110	

Table A.4: Operational Wind Plants in Counties St - Wi

SITE #	County	Modeled Capacity (MW)	Data Review
3005	Starr	237.6	< 1yr
21	Sterling	214.5	
23	Sterling	298.5	
22	Sterling	149.5	
80	Sterling	124.2	
96	Sterling	199.5	
15	Taylor	120.6	
19	Taylor	114	
50	Taylor	213	
51	Taylor	299	
67	Tom Green	155	
64	Upton	79.3	
65	Upton	158.6	
66	Upton	40.3	
38	Val Verde	121.9	
39	Val Verde	27.44	
24	Webb	150	
7	Webb	19.69	
8	Webb	230	
2009	Webb	200	
3009	Webb	300.5	< 1yr
37	Webb	92.34	
2006	Wilbarger	135.4	
33	Wilbarger	230	
3003	Wilbarger	183.75	< 1yr
74	Willacy	200.1	
75	Willacy	201.6	
4	Willacy	228	
103	Willacy	203.29	
90	Winkler	60	
2089	Winkler	92.61	

APPENDIX B – HYPOTHETICAL WIND PLANTS BY COUNTY

Table B.1: Count of Sites and Total Capacity by County

County	#	Cap (MW)	County	#	Cap (MW)	County	#	Cap (MW)
Andrews	2	345.7	Grayson	1	191.8	McMullen	2	350.4
Armstrong	1	383.9	Hall	2	542.2	Menard	2	362.2
Bailey	1	245.3	Hansford	1	400	Midland	2	328.6
Bee	2	323.8	Hardeman	2	311.9	Mills	1	140.2
Bell	1	122.5	Hartley	1	352.1	Montague	2	326.7
Bosque	2	292.5	Haskell	2	434.1	Moore	1	400
Brazoria	1	130.8	Hidalgo	2	454.9	Motley	2	341.2
Brooks	1	154.1	Hill	1	375.1	Navarro	2	414.5
Brown	2	452.1	Hood	1	162.4	Nolan	1	338.6
Calhoun	1	199.8	Hopkins	1	143.1	Ochiltree	1	130.3
Callahan	1	103.5	Hunt	1	237.3	Parker	1	230.6
Castro	1	357.8	Hutchinson	1	271.5	Potter	2	749.1
Childress	1	310.4	Irion	1	208.9	Reeves	1	102.7
Cochran	1	130.8	Jackson	3	617.5	Refugio	1	169.9
Coke	1	212.6	Jefferson	2	247.5	Roberts	2	329.5
Coleman	2	498.8	Jim Wells	1	171.4	Schleicher	1	241
Collin	1	223	Johnson	2	350.3	Scurry	1	311.8
Concho	1	252.2	Jones	1	210.6	Sherman	1	148.9
Coryell	2	409	Karnes	1	158.1	Stephens	2	349.7
Cottle	2	428.1	Kaufman	1	103.9	Stonewall	1	343.2
Crockett	1	254.4	Kendall	1	305.1	Sutton	2	275.3
Crosby	1	400	Kerr	1	126	Swisher	1	176.1
Culberson	1	160	Kimble	1	115.4	Terrell	1	155.4
Dallam	1	222.3	King	2	405.8	Throckmorton	2	422.6
Denton	1	351.4	Kleberg	1	254.9	Travis	1	121.1
Duval	2	455.7	Knox	1	117	Van Zandt	1	183
Eastland	1	105.7	Lamar	1	213.3	Victoria	1	106.5
Ector	1	400	Lamb	1	105.6	Wharton	1	194.2
Ellis	2	560	LaSalle	1	252	Wheeler	2	318.1
Falls	1	167.2	Lavaca	1	185.6	Wichita	1	151.6
Fannin	1	335.6	Limestone	1	229.8	Wilbarger	2	391.2
Fayette	1	151.3	Lipscomb	1	281	Willacy	2	636.9
Fisher	1	130.6	Live Oak	1	187.6	Williamson	1	262.5
Foard	1	308.9	Lubbock	1	150.8	Wise	1	152.9
Gaines	1	108.2	Lynn	1	145.9	Yoakum	1	259.7
Gillespie	1	400	Mason	1	148	Young	1	332.9
Glasscock	2	299.6	Matagorda	1	210	Zapata	2	337
Gray	1	271.2	McLennan	1	246.6	*Total (GW)*	148	30.9

APPENDIX C – OPERATIONAL AND PLANNED UTILITY-SCALE PV PLANTS

Table C.1: Operational and Planned Utility-Scale PV Plants in Counties A - Pe

Site #	County	MW_{AC}	Data Review
29	Andrews	100.7	< 6 months valid
39	Andrews	153.6	< 6 months valid
14	Bexar	39.18	
37	Borden	101.4	< 6 months valid
38	Borden	125.3	< 6 months valid
36	Brazoria	120	< 6 months valid
9	Brewster	50	
12	Childress	121.4	< 6 months valid
27	Crane	152.5	< 6 months valid
10	Dawson	50	
11	Dawson	101.6	
31	Ector	16.8	< 6 months valid
22	Haskell	106.4	
13	Kent	118.6	< 6 months valid
5	Kinney	37.62	
28	Nolan	102.2	< 6 months valid
8	Pecos	7.41	
7	Pecos	22	
21	Pecos	50	
20	Pecos	110.2	

Table C.2: Operational and Planned Utility-Scale PV Plants in Counties Pe - W

Site #	County	MW_{AC}	Data Review
2	Pecos	126	
19	Pecos	155.44	
24	Pecos	182	
1	Presidio	10	
17	Reeves	78.75	
18	Reeves	78.75	
35	Reeves	101.01	< 6 months valid
3	Sterling	30	
25	Travis	26.7	
23	Upton	157.5	
4	Upton	180	
32	Upton	205	< 6 months valid
6	Uvalde	95	
15	Winkler	125.04	< 6 months valid
16	Winkler	127.95	< 6 months valid

APPENDIX D - HYPOTHETICAL PV PLANTS BY COUNTY

Table D.1: Net Capacity Factor for Hypothetical & Queued Sites in Counties A - La

SITE ID	County	NCF Single	NCF Dual
745	Andrews	29.4%	30.2%
5726	Angelina	22.7%	23.4%
2804	Armstrong	27.3%	28.6%
1115	Bailey	29.1%	30.1%
4753	Bee	24.0%	24.5%
4433	Bexar	23.8%	24.3%
1403	Borden	27.9%	28.8%
4051	Bosque	24.5%	25.3%
5922	Brazoria	22.9%	23.4%
30	Brewster	31.6%	31.9%
2695	Briscoe	27.5%	28.7%
3202	Brown	25.8%	26.5%
2864	Callahan	26.3%	27.2%
2740	Cameron	24.9%	25.4%
2946	Carson	27.3%	28.5%
1908	Castro	28.4%	29.5%
3846	Childress	26.0%	27.2%
945	Cochran	29.1%	30.1%
2326	Coke	26.9%	27.8%
2925	Coleman	26.0%	26.8%
3511	Comanche	25.7%	26.5%
2168	Concho	26.3%	27.0%
4971	Cooke	24.0%	24.8%
3415	Cottle	26.5%	27.6%
577	Crane	29.2%	30.1%
805	Crockett	28.2%	28.9%
2101	Crosby	27.8%	28.9%
176	Culberson	31.9%	32.4%
5018	Dallas	23.5%	24.3%
1136	Dawson	28.3%	29.2%
1348	Deaf Smith	28.8%	29.9%
4831	Denton	24.2%	25.0%
2759	Dickens	27.2%	28.2%
1713	Dimmit	25.0%	25.4%
3405	Donley	26.8%	28.1%
2436	Duval	24.2%	24.7%
3116	Eastland	25.7%	26.6%
651	Ector	29.3%	30.2%
1720	Edwards	26.0%	26.6%

SITE ID	County	NCF Single	NCF Dual
4779	Ellis	23.7%	24.4%
4963	Falls	23.6%	24.3%
5516	Fannin	23.3%	24.1%
2173	Fisher	26.8%	27.7%
2560	Floyd	27.8%	28.8%
5961	Fort Bend	23.0%	23.6%
2688	Frio	24.2%	24.7%
831	Gaines	29.2%	30.1%
1980	Garza	27.8%	28.8%
2437	Gillespie	25.5%	26.1%
1008	Glasscock	27.9%	28.7%
5597	Grimes	23.3%	24.0%
2062	Hale	28.0%	29.1%
3399	Hall	26.6%	27.8%
4156	Hardeman	25.6%	26.7%
5718	Harris	23.4%	23.9%
3061	Haskell	26.1%	27.1%
1545	Hidalgo	25.1%	25.6%
4458	Hill	23.9%	24.7%
1238	Hockley	28.6%	29.6%
6003	Hopkins	23.0%	23.8%
1217	Howard	27.8%	28.6%
5790	Hunt	23.1%	23.9%
1117	Irion	27.2%	27.9%
5417	Jackson	23.4%	23.9%
105	Jeff Davis	31.9%	32.4%
1309	Jim Hogg	25.2%	25.7%
4553	Jim Wells	24.1%	24.6%
2638	Jones	26.4%	27.4%
5366	Kaufman	23.3%	24.1%
2154	Kent	27.3%	28.3%
2405	Kerr	25.3%	25.8%
2134	Kimble	25.7%	26.4%
3022	King	26.5%	27.5%
1923	Kinney	25.1%	25.6%
3443	Knox	25.9%	27.0%
2351	La Salle	24.5%	25.0%
6025	Lamar	22.9%	23.7%
1336	Lamb	28.6%	29.6%

Table D.2: Net Capacity Factor for Hypothetical & Queued Sites in Counties Lo - Z

SITE ID	County	NCF Single	NCF Dual
672	Loving	29.8%	30.6%
1992	Lubbock	27.9%	28.9%
1475	Lynn	28.2%	29.1%
1047	Martin	28.1%	29.0%
2346	Mason	25.8%	26.5%
5892	Matagorda	23.2%	23.7%
1715	Maverick	25.3%	25.8%
2279	McCulloch	26.1%	26.8%
4657	McLennan	24.0%	24.7%
2870	McMullen	24.2%	24.7%
3480	Medina	24.1%	24.6%
1999	Menard	26.2%	26.9%
896	Midland	28.4%	29.2%
3397	Mills	25.4%	26.2%
1618	Mitchell	27.3%	28.2%
3062	Motley	27.3%	28.5%
4946	Navarro	23.6%	24.3%
1957	Nolan	27.2%	28.1%
4515	Nueces	24.0%	24.5%
2338	Oldham	28.5%	29.8%
1233	Parmer	28.9%	30.0%
136	Pecos	30.5%	31.0%
3188	Potter	27.6%	28.9%
4	Presidio	31.8%	32.2%
2512	Randall	28.0%	29.2%
906	Reagan	28.1%	28.9%
3236	Real	25.2%	25.7%
439	Reeves	30.5%	31.2%
2548	Runnels	26.3%	27.1%
3005	San Saba	25.6%	26.3%
1487	Schleicher	26.5%	27.1%
2010	Scurry	27.2%	28.1%
3075	Shackelford	26.0%	27.0%
1161	Starr	25.2%	25.7%
3284	Stephens	25.5%	26.5%
1488	Sterling	27.7%	28.5%
2791	Stonewall	26.5%	27.6%
1633	Sutton	26.2%	26.8%
2536	Swisher	27.9%	29.0%
2416	Taylor	26.9%	27.8%
509	Terrell	28.9%	29.7%
1162	Terry	28.6%	29.6%
3225	Throckmorton	25.9%	26.9%
1919	Tom Green	26.7%	27.4%
5044	Travis	23.5%	24.1%
647	Upton	29.0%	29.8%
2723	Uvalde	24.4%	24.9%
736	Val Verde	27.8%	28.5%
5375	Van Zandt	23.3%	24.0%
5198	Victoria	23.5%	24.0%
555	Ward	29.7%	30.6%
1097	Webb	25.2%	25.7%
5804	Wharton	23.2%	23.8%
4671	Wichita	24.9%	26.0%
2916	Willacy	24.7%	25.2%
4927	Williamson	23.7%	24.3%
704	Winkler	29.6%	30.4%
903	Yoakum	29.2%	30.1%
3839	Young	25.2%	26.2%
1158	Zapata	25.3%	25.7%
1914	Zavala	24.6%	25.1%

APPENDIX E - COUNTIES IN ERCOT CDR ZONES

Table E.1: Counties by CDR Zone (Coastal, Houston, North, and Panhandle)

Coastal
Aransas
Brazoria
Calhoun
Cameron
Kenedy
Kleberg
Matagorda
Nueces
Refugio
San Patricio
Willacy

Houston
Chambers
Fort Bend
Galveston
Harris
Montgomery
Waller

North
Anderson
Angelina
Bell
Bosque
Brazos
Brown
Cherokee
Collin
Comanche
Cooke
Coryell
Dallas
Delta
Denton
Eastland
Ellis
Erath
Falls
Fannin
Franklin
Freestone
Grayson
Grimes
Hamilton
Henderson
Hill
Hood
Hopkins
Houston
Hunt
Jack
Johnson
Kaufman
Lamar
Lampasas
Leon
Limestone
Madison

North *(cont.)*
McLennan
Mills
Montague
Nacogdoches
Navarro
Palo Pinto
Parker
Rains
Red River
Robertson
Rockwall
Rusk
San Saba
Smith
Somervell
Stephens
Tarrant
Titus
Van Zandt
Wise
Wood

Panhandle
Armstrong
Bailey
Briscoe
Carson
Castro
Childress
Cochran
Collingsworth
Crosby
Dallam
Deaf Smith
Dickens
Donley
Floyd
Gray
Hale
Hall
Hansford
Hartley
Hemphill
Hockley
Hutchinson
Lamb
Lipscomb
Lubbock
Moore
Motley
Ochiltree
Oldham
Parmer
Potter
Randall
Roberts
Sherman
Swisher
Wheeler

Table E.2: Counties by CDR Zone (South and West)

South
Atascosa
Austin
Bandera
Bastrop
Bee
Bexar
Blanco
Brooks
Burleson
Burnet
Caldwell
Colorado
Comal
DeWitt
Dimmit
Duval
Edwards
Fayette
Frio
Gillespie
Goliad
Gonzales
Guadalupe
Hays
Hidalgo
Jackson
Jim Hogg
Jim Wells
Karnes
Kendall
Kerr
Kimble
Kinney
La Salle
Lavaca
Lee
Live Oak
Llano

South *(cont.)*
Mason
Maverick
McCulloch
McMullen
Medina
Milam
Real
Starr
Travis
Uvalde
Victoria
Washington
Webb
Wharton
Williamson
Wilson
Zapata
Zavala

West
Andrews
Archer
Baylor
Borden
Brewster
Callahan
Clay
Coke
Coleman
Concho
Cottle
Crane
Crockett
Culberson
Dawson
Ector
El Paso
Fisher
Foard
Gaines
Garza
Glasscock
Hardeman
Haskell
Howard
Hudspeth
Irion
Jeff Davis
Jones
Kent
King
Knox
Loving
Lynn
Martin
Menard
Midland
Mitchell

West *(cont.)*
Nolan
Pecos
Presidio
Reagan
Reeves
Runnels
Schleicher
Scurry
Shackelford
Sterling
Stonewall
Sutton
Taylor
Terrell
Terry
Throckmorton
Tom Green
Upton
Val Verde
Ward
Wichita
Wilbarger
Winkler
Yoakum
Young